

Review

Solar Chimney Power Plants for Sustainable Air Quality Management Integrating Photocatalysis and Particulate Filtration: A Comprehensive Review

Dipak Kumar Mandal ¹, Sharmistha Bose ², Nirmalendu Biswas ³, Nirmal K. Manna ⁴, Erdem Cuce ^{5,6} and Ali Cemal Benim ^{7,*}

- ¹ Department of Mechanical Engineering, Government Engineering College, Samastipur 848127, India; dipkuma@yahoo.com
- ² Department of Basic Science, College of Engineering and Management, Kolaghat 721171, India; sharmi08bose@gmail.com
- ³ Department of Power Engineering, Jadavpur University, Salt Lake, Kolkata 700106, India; biswas.nirmalendu@gmail.com
- ⁴ Department of Mechanical Engineering, Jadavpur University, Kolkata 700032, India; nirmalkmannaju@gmail.com
- ⁵ Department of Mechanical Engineering, Faculty of Engineering and Architecture, Recep Tayyip Erdogan University, Zihni Derin Campus, 53100 Rize, Turkey; erdem.cuce@erdogan.edu.tr
- ⁶ School of Engineering and the Built Environment, Birmingham City University, Birmingham B4 7XG, UK
- ⁷ Department of Mechanical and Process Engineering, Düsseldorf University of Applied Sciences, 40476 Düsseldorf, Germany
- * Correspondence: alicemal.benim@hs-duesseldorf.de

Abstract: Urban air pollution has become a pressing challenge in recent times, demanding innovative solutions. This review delves into the potential of Solar Chimney Power Plants (SCPPs) as a sustainable approach to mitigating air pollution. The idea of mitigation of pollution may be an added advantage to the use of SCPPs in practice. Recent advancements, such as the integration of photocatalytic reactors (PCRs) for the elimination of greenhouse gases (GHGs), emphasizing the importance of addressing non-CO₂ GHGs like CH₄ and N₂O are analyzed. The novelty of this review is that it not only focuses on the shifting and removal of particulate matter but also on the removal of greenhouse gases. Numerous case studies, ranging from filter-equipped SCPPs to Solar-Assisted Large-Scale Cleaning Systems (SALSCSs), are reviewed, providing a comprehensive understanding of their design, performance, and potential benefits. This review serves as a guide for researchers and policymakers, emphasizing the need for multifaceted approaches to address the intricate nexus of air pollution, renewable energy generation, and climate change mitigation.

Keywords: solar chimney; air pollution; greenhouse gases; particulate matter; photocatalysis



Citation: Mandal, D.K.; Bose, S.; Biswas, N.; Manna, N.K.; Cuce, E.; Benim, A.C. Solar Chimney Power Plants for Sustainable Air Quality Management Integrating Photocatalysis and Particulate Filtration: A Comprehensive Review. *Sustainability* **2024**, *16*, 2334. <https://doi.org/10.3390/su16062334>

Academic Editors: Fu Gu, Jingxiang Lv and Shun Jia

Received: 6 February 2024

Revised: 4 March 2024

Accepted: 7 March 2024

Published: 12 March 2024



Copyright: © 2024 by the authors. Licensee MDPI, Basel, Switzerland. This article is an open access article distributed under the terms and conditions of the Creative Commons Attribution (CC BY) license (<https://creativecommons.org/licenses/by/4.0/>).

1. Introduction

1.1. Background and Significance

From the extensive smog blanketing cities to the distressing occurrence of premature deaths, all are outcomes of air pollution. Globally, 99% of people breathe air with higher pollution levels than those recommended by the air quality guideline, published by WHO in 2021 [1]. Annually, 6.7 million premature deaths result from the combined effects of indoor and outdoor air pollution. In 2019, the deaths because of outdoor air pollution were 4.2 million, and 89% of these premature deaths occurred in low- and middle-income countries [2]. The air pollution problem is more significant in developing countries in the cities, especially ones with high populations. During the past few years, the air quality in many cities in India has worsened, and serious haze problems are being experienced, particularly in the winter season. Apart from health effects, air pollution caused by greenhouse gas emissions leads to global warming and subsequent climate change. Moreover,

the abundance of aerosols in high concentrations contributes to the development of haze in the atmosphere. This phenomenon can have far-reaching effects on both local and global climates by altering the hydrological cycle, hindering monsoon circulation, and diminishing local precipitation [3,4]. It is believed that in China, the main reason for the recent southward migration of the summer monsoon belt is the significant increase in atmospheric aerosol [5,6].

Air pollution arises from both human-made sources and natural occurrences such as volcanic eruptions, dust storms, and wildfires. Fossil fuel combustion stands out as a significant anthropogenic contributor to air pollution. This is a principal contributor to greenhouse gas emissions like CO₂, oxides of nitrogen, and the atmospheric release of particulate matter that not only has tremendous health effects but also results in haze and visibility deterioration [7,8]. To control the rise in temperature, which should be kept to 1.5 °C as per the Paris Agreement of 2015, and at the same time to meet the energy demand, each country has proposed several strategies for an overall scaling down of greenhouse gas (GHG) emissions, which include improvement in energy conversion processes, the introduction of incentives for renewable energy generation, carbon taxes, etc., as well as the introduction of decarbonization technologies [9]. In the European Union, 38% of the electricity consumption was generated by renewable energy sources in the year 2020 [10]. Globally, the electricity sector can potentially be 100% renewable energy-based by 2030 and will be the first fully decarbonized sector according to governmental plans and visions [11,12].

Within the array of renewable energy sources, solar energy-based SCPPs emerge as a promising low-carbon emission technology, generating electricity through the creation of an air draft via solar heating and a chimney. The air from the atmosphere entering through the solar collector is heated inside the solar collector and rises upwards through the chimney as its density decreases with temperature. The hot low-density air drives the turbine during its upward movement. The running process by the generated air flow and energy transformation is represented in Figure 1. This technology is sustainable, reliable, and requires low maintenance. One of the major constraints of the wide-scale use of SCPPs is their low conversion efficiency. A recent study reveals that the technology of SCPPs can also be used to reduce GHGs and to arrest particulate matter from the atmosphere, which ultimately facilitates an improvement in the urban air quality along with the production of clean and sustainable energy. Utilizing a hybrid SCPP can offset the lower conversion efficiency that is observed in the original SCPP, consequently enhancing the overall performance of the system.

1.2. Air Pollution and GHG Emission

Air pollution is not a recent phenomenon. In ancient times, the consequences of air pollution were limited to a particular area. In 1307, King Edward I banned the use of coal in lime kilns in London. The problem of air pollution was aggravated with the industrial revolution, as the demand for coal usage increased in industrial sectors like power plants, smelting, steel, etc. Several air pollution episodes of the last century (Table 1) were primarily the result of exceptionally high concentrations of sulfur oxides and particulate matter that were emitted due to the combustion of coal.

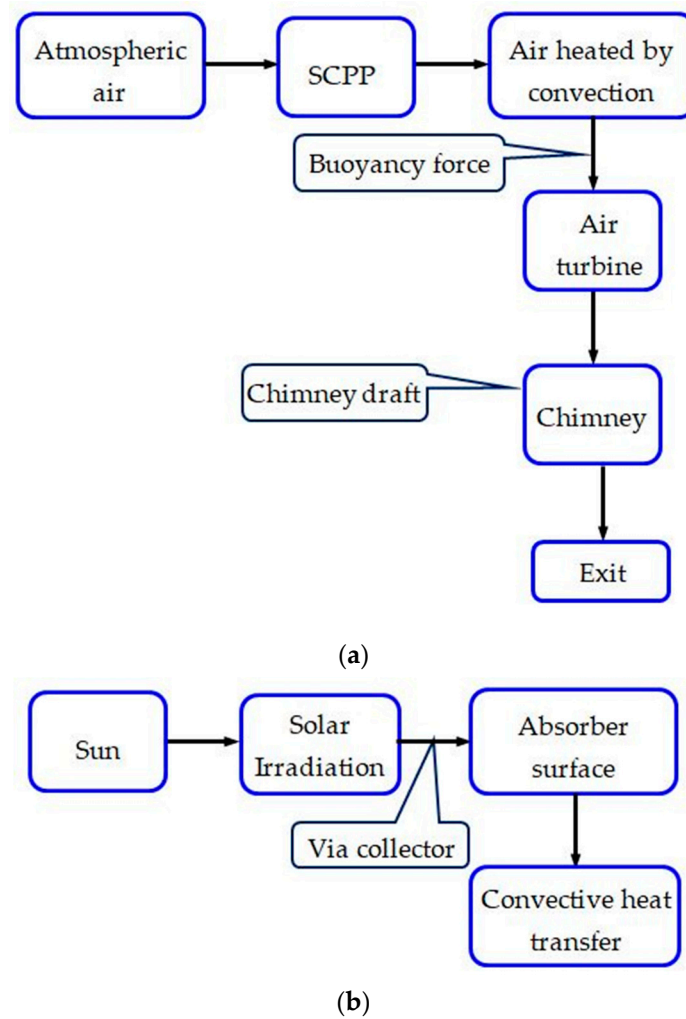


Figure 1. Energy flow and developed airflow phenomena in SCP. (a) Air flow; (b) Energy flow.

Table 1. Overview of significant air pollution episodes associated with traditional industries [13].

Episode	Year	Source	Result
Meuse Valley, Belgium	1930	Densely populated factories such as zinc smelter, glass, and steel manufacturing industries	Severe respiratory symptoms, death of 63 people, illness of approximately 6000 residents
Gas attack, Los Angeles	1940	Auto exhaust and petroleum refineries	Severe air pollution problem
Donora, Pennsylvania	1948	High concentrations of HCl emitted from zinc smelting and blast furnaces	20 deaths and 600 people becoming ill
Great London Smog	1952	Coal combustion in power plants	4000 deaths in a week
Los Angeles Smog	1954	Dense photochemical smog resulting from a combination of VOC, NO _x , and sunlight	2000 auto accidents in a single day
Acid rain, America	1969	Sulfur dioxide emission from industries	Burned lawns, ate away tree leaves, and damaged feathers of birds

A recent special report on keeping global warming to 1.5 °C states that excess concentration of greenhouse gases like CO₂, CH₄, N₂O, O₃, CFC, and H₂O in the atmosphere is primarily accountable for climate change [14]. Again, climate change is the manifestation of air pollution. In the last few decades, the global climate pattern has been changing, and the world is facing more frequent natural disasters like extreme temperature events

(ETEs), droughts, and floods [15,16]. Global monsoon drizzle is expected to increase by $1.71 \pm 2.38\%$ in 2021–2040 under the high climate change scenario [17], and the frequency of floods will be 4–14 times higher by 2100 compared to the 1971–2000 average [18]. Global warming accompanied by the melting of glaciers and ice sheets will also lead to a rise in sea levels. If the greenhouse gas emission prevails in its present form, the sea water level will be 75 cm higher by 2100 than the average sea level height from 1986 to 2005 [19].

The relation between climate change and humans is presented in Figure 2. As seen in Figure 2, climate change not only affects the physical environment but also affects human health and well-being through several pathways. Climate change and air pollution are interconnected, and one amplifies the impact of the other. Climate change-induced heat waves, storms, and wildfires aggravate the air pollution problem. A high temperature enhances the growth of the photochemical reactions between the ground-level ozone-forming precursors and thus results in an increase in ground-level ozone formation [20], which is responsible for eye and throat irritation and a reduction in the yield of major crops like corn, wheat, soybeans, and peanuts. Wildfire causes the emission of vast quantities of particulate matter and black carbon that can traverse long distances and thus deteriorate the global air quality. Globally, more than 90% of children below the age of eighteen breathe air where the pollutant level exceeds the tolerable limit specified by the WHO. Infant mortality, asthma, neuro-developmental disorders, and childhood cancers can all be linked to the unfavorable health effects of air pollution. Air pollution is the second leading cause of many alarming non-communicable diseases like stroke, cancer, and heart disease, according to a WHO report from 2022 [2]. In 2019, more than 3 million people died worldwide from COPD connected to air pollution and climate change [21,22].

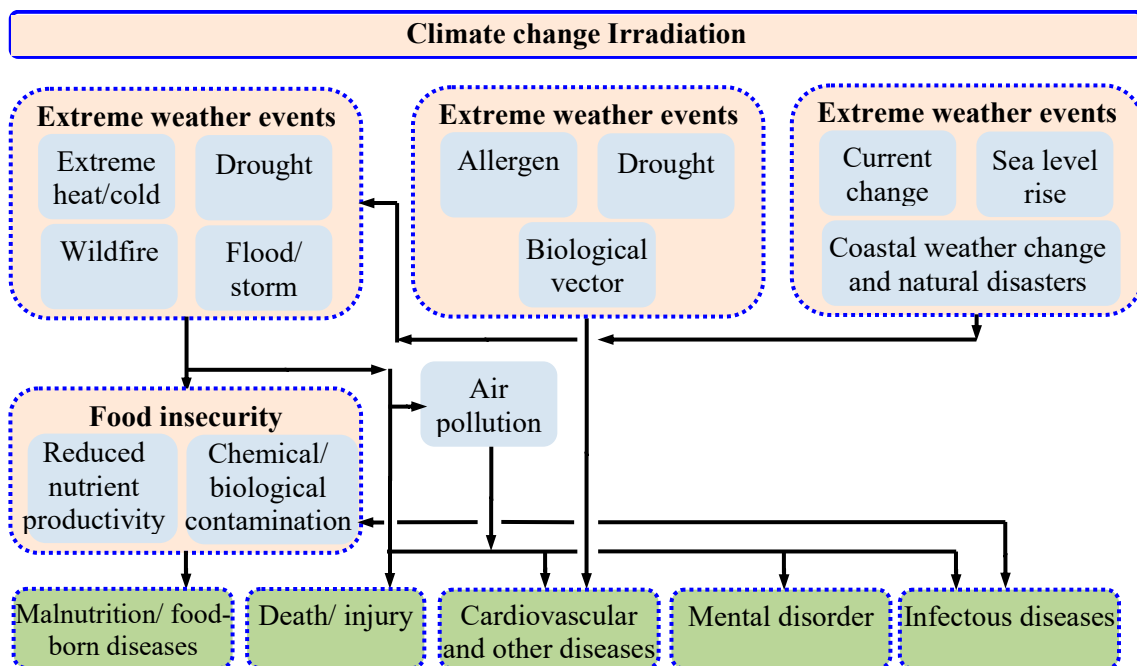


Figure 2. Effect of climate change on humans [23].

1.3. Air Pollution and Particulate Matter Concentration

Air pollution due to particulate matter is now an important issue in megacities of developing nations. Traffic emissions, mainly particulate matter (PM_{2.5}) and oxides of nitrogen, are the main origin of air pollution in city air, and the concentrations of these pollutants in street environments are high [24,25]. It is observed that pedestrians on high-density urban streets are 30 times more exposed to ultrafine particles per trip than people driving with closed windows [26]. This is because pollutants that are nearer to the surface do not disperse easily owing to the urban spatial form [27,28] and assorted materials in the

urban space [29]. This problem becomes more severe when pollutants accumulate near the surface due to a low or no wind speed [30]. In the USA, every year, 53,000 people die early due to vehicle discharges [31]. In 2015, 4.2 million people died from exposure to PM_{2.5}, and 59% of these were from East and South Asia [32]. Several research works show that exposure to particulate matter with a diameter of 10 microns and 2.5 microns or less leads to a higher risk of lung cancer [33,34] and several respiratory diseases, including COPD and allergic rhinitis. Every 10 µg/m³ increase in PM_{2.5} concentration causes a 1.12-fold increase in COPD mortality [35]. Globally, subjection to ambient fine particles is enlisted as being eighth among the leading death-causing risks [36].

Apart from health effects, atmospheric aerosol consisting of particles with an effective diameter of less than 10 µm influences the regional and local climate directly and indirectly. The incident sunlight can be scattered and absorbed by the atmospheric aerosol. Thus, a high concentration of particulate matter in the air becomes a cause of haze formation and visibility reduction [7,8]. Recently, this weather phenomenon has been noticed in many countries [37–40]. In addition to this function, aerosols serve as surfaces for cloud droplet condensation. Consequently, atmospheric clouds undergo a transformation into smaller droplets, causing an extended retention of water in the atmosphere. This, in turn, results in a reduction in the precipitation rate over an extended period.

Governments have implemented various measures to regulate the concentrations of particulate matter in urban air. These initiatives include enforcing the mandatory installation of air pollution control devices in industries that release particulate matter and setting emission limits for vehicles. In major metropolitan cities in China, the government has not only imposed traffic restrictions but also curtailed operations in industries emitting air pollutants in large quantities [5]. In Delhi, the capital and one of the major metropolitan cities of India, the air quality has worsened in the past few years. One of the major air pollutants that is responsible for deteriorated air quality is the high atmospheric concentration of particulate matter. To curb pollution levels, the government must ban different activities like the entry of polluting trucks, commercial four-wheelers, non-essential construction works, etc. While the existing measures provide a temporary reduction in the airborne particulate matter concentration, addressing these issues necessitates the implementation of long-term strategies for a sustained improvement in air quality. Table 2 shows the updated AQG levels for particulate matter as per the WHO [41].

Table 2. Recommended 2021 AQG (air quality guideline) levels compared to 2005 air quality guidelines [41].

Pollutant	Averaging Time	2021 AQGs	2005 AQGs
Particulate matter of 2.5 micron	Annual	5	10
	24 h *	15	25
Particulate matter of 10 micron	Annual	15	20
	24 h *	45	50

* 99th percentile (i.e., 3–4 exceedance days per year).

1.4. Scope and Objectives of This Study

Review studies provide a concise overview of prior research, serving the interests of non-experts and current researchers in relevant fields. Regarding SCPPs, 19 review papers have been noted and cited in this study. The majority of these studies focus on fundamental concepts and advancements that are aimed at enhancing both the power generation and efficiency. Many papers are based on the basic principles, advantages, and disadvantages of SCPPs [42–45]. The impact of geometry modification on a plant's performance is studied by many studies [46–48]. A few articles [43,49] describe the innovations in this field while considering different locations. The study of optimization, exergy analysis, and commercialization is reported on by different researchers [47,49,50]. Additionally, various papers explore hybrid systems to enhance the efficiency of a system [51,52]. Chikere et al. [53]

focused on using waste gas for thermal energy to enhance the overall performance of plants. Since the discussion of experimental work in a review paper is very sparse, Biswas et al. [54] studied the experimental works in their review paper. Sharon et al. [55] carried out an exhaustive study of the detailed application of solar chimneys. They studied different hybrid power plants by using waste gas, geothermal energy, PV cells, solar stills, desalination, etc., to enhance the time needed for power generation and the overall utilization of the plant. Despite huge efforts, the improvements in the power and efficiency of SCPPs are not too noteworthy after a lot of geometry modifications and hybridizations. Researchers are currently investigating alternative applications for the plants' utilization. The first review paper to mitigate air pollution by using solar chimneys was written by Liu et al. [56]. They nicely presented the various strategies to mitigate air pollution in a locality. But mostly, they concentrated on removing or transporting the particulate matter into higher or other regions. The current study concentrates on an in-depth analysis of particulate matter and extends its focus to include the removal of greenhouse gases.

The present study contributes significantly to sustainable air quality management by using SCPPs. The significance of the present study is that it addresses the pressing need for sustainable energy solutions by exploring the integration of SCPPs. This seeks to contribute to enhanced air quality management by incorporating photocatalysis and particulate filtration to reduce pollutants that are emitted during power generation. With respect to the global environmental impact, this research aims to offer insights into a holistic approach to power generation that not only produces clean energy but also mitigates airborne pollutants. This involves a detailed examination of the catalytic process and its impact on the degradation of harmful airborne substances. This study aims to identify and analyze the most efficient and sustainable particulate filtration technologies for optimal air quality management. This involves exploring innovative engineering solutions by optimizing SCPPs that maximize the utilization of solar energy while minimizing their environmental impact. Based on the findings, it provides recommendations for implementation and offers practical implementation of SCPPs with integrated air quality management technologies.

In the subsequent sections, this paper delves into analyzing innovative engineering solutions that have been applied to optimize SCPPs. A thorough assessment of the photocatalysis component in SCPPs is described, along with an analysis of the efficiency of the catalytic process in degrading airborne pollutants. Identifying and scrutinizing various particulate filtration technologies, and assessing their efficiency, sustainability, and adaptability to the power plant's design regarding the overall air quality management strategy, is addressed. Examining the environmental and economic implications of the reduction in emissions, the overall cost-effectiveness of the project and potential long-term benefits are discussed. Lastly, future recommendations are provided, including an air quality management system that offers practical implementation of SCPPs.

2. Solar Chimney Power Plants: An Overview

2.1. Principles and Running of SCPPs

An SCPP is expansive in size, but its operational physics are straightforward, making it easy to convert thermal energy into electrical energy. Construction-wise, there are four main components, the collector or canopy, absorber, chimney, and air turbine (Figure 3). The phenomenon of free convection generates air flow in the SCPP. Radiation energy coming from the sun falls on the bottom absorber via a transparent collector, causing heating of the black absorber wall. Convective heat transfer causes heating of the air that is adjacent to the absorber wall. The developed buoyancy force helps move the hot air toward the chimney inlet, and therefore, the cold air enters from the inlet of the SCPP. The flow is propelled by the draft of a chimney, located at the center of the SCPP. The generated kinetic energy of the air is utilized by an air turbine at the entry to the chimney and converts mechanical energy into electrical using a generator. Finally, the hot air exits via a chimney outlet [57,58].

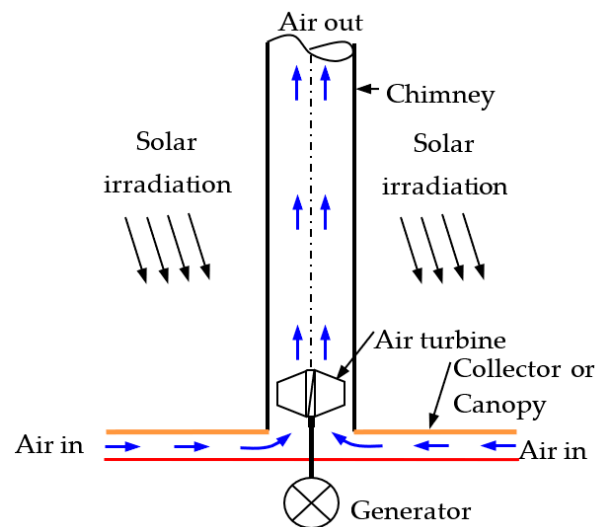


Figure 3. Different components with air flow directions in SCPP.

2.2. Historical Development and Evolution of SCPP

The concept of utilizing heated air from a chimney or fireplace to power a windmill was originally suggested by the renowned Leonardo da Vinci (1452–1519) [59–61]. After a century, the idea of the first SCPP was presented by Spanish artillery colonel Isidoro Cabanyes in 1903, in which heat was taken from a heat exchanger located at the chimney base. A wind wheel was situated at the top of the house to produce electrical energy [62,63]. In 1926, Prof. Dubos utilized the slant of a mountain for an SCPP in North Africa. The SCPP concept with a chimney was reported by Hanns Günther in 1931 [64,65].

In 1980, Prof Schlaich and his group made the prototype for a pilot plant for an SCPP in Manzanares, Spain (Figure 4), which was sponsored by the German Government in collaboration with the Spanish Utility Union ElectricaFenosa [66–70]. This (dimensions: chimney diameter = 10.16 m, chimney height = 194.6 m, collector diameter = 244 m, and collector inlet = 1.85 m) plant was installed, and the generated power amounts to 50 kW.



Figure 4. View of Manzanares plant prototype [49] (adapted with permission from Elsevier).

Cao et al. [71] proposed a chimney for the large-scale cleaning of air. The system consists of an air filter at the entry to the chimney to remove particulate matter of more than or equal to 2.5 μm . Numerous studies, such as those conducted by Zhou et al. [72] and Ming et al. [73], have suggested the dispersion of warm air to higher altitudes, possibly within the upper layer of the troposphere, as a strategy for mitigating haze dispersion. Additionally, various investigations on small-scale solar chimneys (SCs) aimed at facilitating natural ventilation have been documented, including works by Jing et al. [74] and Khanal and Lei [75].

2.3. Advantages and Challenges of SCPPs

SCPPs are promising systems for sustainable and renewable energy generation, possessing numerous advantages, as outlined below:

- (a) They harness abundant solar energy, serving as an environmentally friendly energy source.
- (b) They are straightforward and efficiently produce power, reducing pollution hazards and costs.
- (c) There is no requirement for extensive infrastructure, and plants can be installed on any land, anywhere.
- (d) Repurposing an abandoned thermal power plant's chimney after its operational life incurs minimal costs.
- (e) They require minimal maintenance and have a long lifespan of approximately 80 years.
- (f) The costs of power generation are relatively low compared to other types of plants.
- (g) Furthermore, this type of plant produces no pollution, pollutants, or greenhouse gases, unlike fossil fuel plants.

Despite numerous advantages, these plants encounter certain challenges that have restricted their widespread adoption:

- (a) Constructing these plants necessitates a significant land area, which can occasionally present challenges in densely populated areas.
- (b) The rate of energy production is notably lower compared to traditional power plants.
- (c) The initial investment costs are elevated in comparison to the rate of power generation.
- (d) Extended payback periods are associated with the system.

In the face of these challenges, comprehensive research is underway to enhance the production of clean power, while also optimizing plant utilization. The government also supports the initial cost of installation. Again, a lot of research is being conducted to modify the plant, aiming at some method for alternative utilization.

Traditional fossil fuel-based power plants release pollutants, contributing to environmental degradation. On the other hand, SCPPs release no pollutants when equipped with air quality management features, resulting in lower emissions and a reduced environmental impact. While wind turbines generate renewable energy, their output is dependent on variable and less predictable wind speeds compared to the steadiness of solar energy. The location for the turbine is chosen at a high air velocity zone. Photovoltaic panels may experience output fluctuations due to adverse weather conditions and daylight variations. SCPPs, not relying on fossil fuels, offer a more consistent power output due to a steady heat differential. In contrast, natural gas power plants contribute to pollution by depending on fossil fuels. Biomass-based power generation is considered renewable, yet it releases particulate matter and emissions during combustion. Hydropower dams involve significant land use changes and potential environmental impacts. Their location is also dependent on water availability. Geothermal power plants are also location-dependent and viable only in specific geological regions, while SCPPs can be designed in various sizes and adapted to different locations.

Opting to construct a new SCPP rather than retrofitting a traditional plant is influenced by several factors such as incorporating the latest technological advances in solar

chimney technology, designing for optimization, assessing the lifecycle costs, considering the environmental impact, and ensuring site suitability.

2.4. Modifications of SCPPs

Enhancing the standalone SCPP's performance has been a focus for researchers, who have explored modifications to its geometry. Primarily, adjustments have been made to the collector's diameter and height, as well as the slope, along with modifications to the chimney's diameter, height, and shape. An increased height of the chimney causes a rise in performance [76–78], but there is a limitation. Performance enhancement with an increase in the chimney diameter is also noted but only up to some optimum value [79–81]. The impact of the chimney's shape has been noticed by different researchers. Different chimneys show better performance with some optimum magnitude of different angles [82,83]. Besides the highly conductive material of the absorber plate, the nature of the surface also significantly influences the output of the plant. Different designs like wavy, staircase, and bottom triangular designs are also reported [84–86].

The enhancement in efficiency is not especially notable following geometry modifications. In addition, power cannot be generated at night. Therefore, SCPP hybridization is carried out in many ways like using solar PV cells, geothermal, biomass, waste gas, heat exchangers, solar ponds, etc. The waste gas coming from any industry is used to pass below the absorber plate or directly mix with air, and this helps with high air temperatures and achieves power generation in cloudy conditions or at night [87–89]. The integration of photovoltaic cells on the collector increases the power and efficiency of both plants [90–94]. The waste flue gas from biomass and geothermal is used in SCPPs [95–97]. Directly extracting hot water from a solar pond, it is sprayed into the chimney to heat the air beneath the turbine, thereby enhancing the overall efficiency of the plant [98,99]. Utilizing a desalination unit has gained popularity in SCPPs for the separation of pure water from saline water [100–102]. To enrich the performance of an SCPP, a cooling tower is integrated to supply heat into the air [103,104].

3. Mitigating Air Pollution with SCPPs

Numerous researchers, including Khanal and Lei [105], Nasri et al. [106], and Vargas-Lopez et al. [107], have conducted studies on solar-assisted solar chimneys to improve the air quality in residential buildings. Various adaptations of solar chimneys have been employed in the past to facilitate building ventilation, as noted by Maghrabie et al. [108]. This technology serves as a means to transfer heat from the Earth's surface to the troposphere, ultimately contributing to a reduction in the planet's temperature. Recent findings indicate that Solar Chimney Power Plants (SCPPs) can serve as a solution to mitigate ambient air pollution. Researchers have proposed several modifications to SCPPs to address urban air pollution and combat global warming.

3.1. Mitigation Strategies by Coupling SCPPs with Photocatalytic Reactors (PCRs)

In 2013, Richter et al. pointed out that an SCPP is not only a source of clean renewable energy but can also be used to reduce atmospheric GHGs by being combined with photocatalytic technology. It has the potential to act as a bigger photocatalytic reactor. The unique ways in which an SCPP can act as a photocatalytic reactor are as follows:

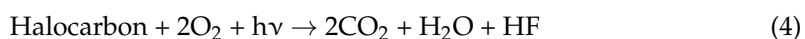
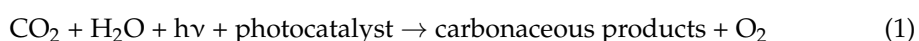
- A large irradiated SCPP greenhouse collector roof can be the source of energy for a photocatalytic reaction.
- A huge area under the SCPP greenhouse collector maximizes the light photocatalyst's illumination area.
- The SCPP facilitates the exposure of the highest volume of flowing polluted air to the photocatalyst by allowing them to come into contact.

In addition to these, the external structure of an SCPP also provides shelter for photocatalytic beds from rain. Thus, a combination of two breakthrough technologies, solar chimneys and photocatalysis, can be a significant approach to mitigating air pollution.

3.1.1. Potential of Photocatalysis in GHG Removal

Research on the photocatalytic degradation of air dates back to the 1970s, when a study was conducted using desert air collected from dust clouds. The result was consistent with the hypothesis that desert regions may be acting as a sink for several atmospheric trace gases [109,110], as SiO₂ is present in sand molecules and acts as a photocatalyst. In 2015, George et al. [111] mentioned in their report that heterogeneous photocatalysis has great potential in the mineralization of some greenhouse gases, thereby reducing global warming. In 2011, de_Richter and Caillol [112] reported a review focusing on the removal of GHGs from the atmosphere by the application of photocatalysis at room temperature to slow down global warming. Recently, visible light-induced heterogeneous photocatalysis has gained interest in the field of GHG removal owing to its inherent advantages. For instance, (i) it harnesses green and sustainable solar energy, (ii) it operates under mild reaction conditions like room temperature and ambient pressure, (iii) it can coat nearly any surface with photoactive materials, and lastly, (iv) it achieves complete mineralization of pollutants. Photocatalysis involves an oxidation and reduction environment, where electron–hole pairs generated from the photocatalyst upon exposure to a light source provide desired reactions depending on the relative locations of the conduction and valance bonds of the semiconductor photocatalyst and the redox level of the substrate (contaminant species). In 2013, de_Richter and Caillol [113] also conducted another review focusing on the removal of GHGs from the atmosphere by the application of photocatalysis at room temperature to slow down global warming.

Photocatalysis of major GHGs proceeds according to the following reactions [112,114]:



Already oxidized molecules like CO₂ and O₃ can only be reduced, whereas reduced molecules like CH₄ can only be oxidized. On the other hand, N₂O can be reduced to N₂ or oxidized to HNO₃, and some members of the CFC family will be oxidized, while some will be reduced, depending on the reaction conditions.

3.1.2. Types of Photocatalysts

(a) Photoreduction of CO₂:

Solar energy-mediated heterogeneous photocatalysis of CO₂ is a promising route for converting atmospheric CO₂ to several value-added C₁/C₂ chemicals like CO, methane, methanol, formic acid, and ethanol. CO₂ can be recycled through this process of artificial photosynthesis and transformed into fuels like methanol and ethanol. The CO₂ photocatalytic reduction pathway proceeds through multiple steps involving the formation of several intermediates, and the formation of end products depends on the reduction potentials of the materials involved [115].

The photocatalysis of CO₂ using dispersed ruthenium and ruthenium oxide on TiO₂ at room temperature and atmospheric pressure was first reported by Thampi et al. [116]. Immediately after that, many works came out describing the photocatalysis reduction of CO₂ with H₂O at room temperature using different compositions of TiO₂ catalysts [117,118]. The work on the photocatalytic decomposition of CO₂ using TiO₂ from 1994 to 2007 was reviewed by Koci et al. [119]. It was seen that the most widely used catalyst for the photoreduction of CO₂ is TiO₂ and its derivatives, and the products are generally methane or methanol.

Recently, lots of studies have been carried out on the photocatalytic reduction of CO₂ using different materials (Table 3) such as photocatalysts [120–122]. These materials can be grouped in the following way:

- Metal–organic framework (MOF)-based photocatalysts: Efficient at capturing and activating CO₂, good absorber of light, and the well-defined and tailored structure of MOFs is advantageous for understanding the mechanism clearly [123,124].
- Covalent organic framework (COF)-based photocatalysts: Currently, this group of compounds is attracting significant attention for the photocatalytic conversion of CO₂ due to several characteristics like chemical stability, an effective charge separation ability, and a high surface area that promotes the harvesting of light, chemical stability, and an effective charge separation ability [125,126].
- Bi-based photocatalysts: These materials exhibit a strong light-absorbing capability owing to their narrow band gap [127].
- g-C₃N₄ and other polymeric semiconductors: These types of photocatalysts have been developed mainly for the photocatalytic conversion of CO₂ into fuels. They are designed in a way so that they can facilitate the electron–hole separation that is required for the photocatalytic conversion of CO₂ [128].
- TiO₂-based photocatalysts: These are the most studied photocatalysts for the photocatalytic reduction of CO₂.

Table 3. Examples of recent MOF-, COF-, and g-C₃N₄-based photocatalysts for CO₂ reduction.

Authors	Photocatalyst	Observations	Main Product
Lee et al. [129]	Zr/Ti-MOF	Mixed-ligand strategy introducing a new energy level in the band structure of the metal–organic frameworks, which increases the photocatalytic activity of the MOF.	HCOOH
Huabin et al. [130]	MOF-525-Co	Presence of a single CO atom in the metal–organic framework enhances the electron–hole separation efficiency in Porphyrin units.	CO, CH ₄
Fu et al. [131]	N ₃ -COF	Azine-based covalent organic frameworks can be an ideal metal-free semiconductor.	CH ₃ OH
Lu et al. [132]	DQTP COF-Co	The introduction of transition metal ions in COFs exerts a strong influence on the selectivity of products (CO or HCOOH). For example, for DQTP COF-Zn, the HCOOH production rate is higher.	CO
Wang et al. [133]	BiOI/g-C ₃ N ₄	Synthesized composite showing higher photocatalytic activity than pure g-C ₃ N ₄ and BiOI.	CO, CH ₄
Xia et al. [134]	Ultrathin g-C ₃ N ₄ nanosheets	Exhibits better performance than unmodified conventional g-C ₃ N ₄ photocatalysts.	CH ₄ , CH ₃ OH
Kumar et al. [135]	Nanoporous g-C ₃ N ₄ /Ir-T	Higher yield of methanol (9934 μmol g ^{−1} cat) compared to semiconductor carbon nitride (145 μmol g ^{−1} cat) after 24 h irradiation.	CH ₃ OH

(b) Photo-oxidation of CH₄:

From 1972 to 1974, Formenti et al. [136] and Djeghri et al. [137] studied the photo-oxidation of linear and branched chain alkanes at room temperature. They used the anatase form of TiO₂ and UV radiation (210–390 nm) as a source of photo radiation for their study. Kaliaguine [138] used vanadium derivatives for his study. However, TiO₂ and its derivatives were used by most scientists to study the kinetics of methane, ethane, and alkenes. Table 4 shows examples of photocatalysts that were used for the total oxidation of methane in different studies.

Table 4. Examples of photocatalysts used for photo-oxidation of CH₄.

Authors	Photocatalyst	Observations	Main Product
Krishna et al. [139]	Uranyl-anchored MCM-41	Focus was on the photo-oxidation of CH ₄ to CO ₂ at room temperature under sunlight.	CO ₂
In et al. [140]	TiO ₂ nanotube arrays	Photocatalyst thickness was about 575 nm, and the illumination wavelength was 367 nm.	CO ₂
Pan et al. [141]	SrCO ₃ /SrTiO ₃	Conversion rate up to 100%. Also applicable to low-concentration methane.	CO ₂
Chen et al. [142]	Silver-decorated ZnO-nano catalyst	Shows great prospects for atmospheric methane oxidation by simulated sunlight illumination.	CO ₂
Wei et al. [143]	Ga ₂ O ₃ and activated carbon with a mass ratio 3:17	Conversion rate of 91.5% after 2.5 h.	CO ₂
Li et al. [144]	Nanosheets and nanorods of ZnO	Focus was on the degradation of low-concentration methane (200 ppm). Conversion rate of 80% after 2 h.	CO ₂
Li et al. [145]	CuO/ZnO	Conversion rate of up to 100%.	CO ₂
Chen et al. [17]	Ag/ZnO	Conversion rate of up to 100%.	CO ₂
Brenneis et al. [60]	Copper-treated zeolite particle heated to 310 °C	Removed all atmospheric methane with a concentration of 2 ppm to 2%.	CO ₂

(c) Photoreduction of N₂O:

The photodecomposition of N₂O to N₂ and O₂ was first studied by Ebitani et al. [146–148]. The catalyst used was Cu-exchanged ZSM-5 zeolite at 278 K. In 1998, Kudo et al. [149] reported the photocatalytic decomposition of N₂O at room temperature in the presence of water and methanol vapor using Ag- and Cu-supported TiO₂ powder. Later, Matsuoka and Anpo [150] found that zeolites incorporating oxides of transition metals (Ti, V, Mo, Cr) or transition metal ions (Cu⁺, Ag⁺) exhibit high photocatalytic activities for the photocatalytic decomposition of N₂O into N₂ and O₂ and also for CO₂ with H₂O into the products methane and methanol. They also used a Cu⁺ ion in combination with various oxides for the decomposition of N₂O for their study. All these experiments were carried out on a laboratory scale. Field experiments were first carried out by Guarino et al. [151]. They coated Pig house walls with paint containing TiO₂ photocatalysts and observed a reduction of 4% in N₂O levels under the following operating conditions:

Air ventilation flow rate: 780–6690 m³ h⁻¹.

Relative humidity: 52%.

Area of walls painted: 150 m² with 70 g m⁻² TiO₂ paint. Table 5 shows a review of different works on the photoreduction of N₂O.

Table 5. Examples of photocatalysts used by other authors for photoreduction of N₂O.

Authors	Photocatalyst	Observations	Product
Matsuoka et al. [152]	Ag ⁺ /ZSM-5 zeolite	Photoexcitation of the Ag ⁺ – N ₂ O complexes has a significant role in the decomposition of N ₂ O to N ₂ and O ₂ .	N ₂ + 1/2 O ₂
Ju et al. [153]	Ag ⁺ /ZSM-5 zeolite	Photoexcitation of the Ag ⁺ – N ₂ O complexes has a significant role in the decomposition of N ₂ O to N ₂ and O ₂ .	N ₂ + 1/2 O ₂
Rakhmawaty et al. [154]	Ti/USY zeolite	A 100 W high-pressure Hg lamp was used for irradiation, and the reaction was carried out at room temperature.	N ₂ + CO ₂
Koci et al. [155]	Ag-TiO ₂ powder	A reaction was carried out in an annular batch reactor at 298 K. An 8 W Hg lamp was used for irradiation. Wavelength of irradiation: 254 nm. After 24 h, 77% conversion of N ₂ O was obtained, with TiO ₂ having 3–4 wt% Ag.	N ₂ + 1/2 O ₂
Koci et al. [156]	TiO ₂	A reaction was carried out in an annular batch reactor at an ambient temperature. The source of irradiation was a Hg lamp. Wavelength of irradiation: 254 nm.	N ₂ + 1/2 O ₂
Matejova et al. [157]	TiO ₂ powder and Cerium-doped TiO ₂	The addition of cerium to TiO ₂ shifts the light absorption range of TiO ₂ from UV to the visible region.	N ₂ + 1/2 O ₂

(d) Photocatalysis of halocarbons:

The photodegradation of HFC and HCFC on several semiconductor metal oxides was studied by Tanaka and Hisanaga [158]. CO_2 , Cl^- , and F^- were the main reaction products, and the performance of the catalyst according to the rate of degradation was in the order of $\text{TiO}_2\text{-ZnO} > \text{Fe}_2\text{O}_3\text{-kaolin}$. Tennakone and Wijayantha [159] reported the photocatalytic mineralization of CFC with fine crystallites if TiO_2 was under UV radiation. The products that were formed were CO_2 , Cl^- , F^- , and Cl_2 . Thereafter, many scientists [160] have studied the photodegradation of halocarbons under different reaction conditions. In most cases, the photocatalyst used was TiO_2 in different forms (crystallites, powder, aqueous suspension) or as its derivatives.

The aforementioned study reveals that TiO_2 stands out as the preferred photocatalyst for the majority of photoreactions. This is due to its high photosensitivity, non-toxic nature, low cost, and chemical stability. But it is UV-active because of its wide band gaps, which creates a barrier to utilizing the solar light effectively, as only 5% of solar light is UV. To resolve this problem efforts have been made to extend the absorption range of TiO_2 to a visible region, which includes transition metal ion doping, non-metal ion doping, metal deposition, semiconductor composites, and conjugated polymer modifications.

3.2. Mechanical Separation of Particulate Matter

Air pollution due to particulate matter is a severe problem in urban areas. SCPPs can be used to mitigate urban air pollution with slight modifications. The separation of particulate matter from air can be achieved in different ways:

- The solar chimney raises polluted air to elevated altitudes.
- The integration of a filter at the entry to the collector inlet aids in air purification.
- Spraying water either inside the chimney air or at the chimney exit contributes to the purification process.

The polluted air passing through the large chimney can be exhausted to the troposphere level above the planetary boundary layer. This reduces ground-level pollution and is applicable in high-haze areas, especially in cities. This is a method that transfers the polluted matter to some zones rather than removing the pollutants. When the chimney height is insufficient, these pollutants will linger in the lower zone, posing a potential risk to human health. Therefore, the concept of the filter is added at the entry that separates very small PM and exhausts clean air into the atmosphere. In this case, if the clean air is sent to the troposphere, there is no use of clean air. This again becomes meaningless, because if the chimney is smaller, then clean air can be used, but the suction action of a short chimney will be significantly reduced, especially as pressure loss occurs at the filter. Then, to use the clean air, a downdraft chimney can be used. This air is again scavenged by cooling water or a cooling tower or heat exchanger. The aerosol that is present in the air is scavenged by the water droplet passing through the hazy air, and then cleans the air. The mechanism of scavenging involves Brownian diffusion, diffusiophoresis, and thermophoresis. Spraying water both in summer and winter improves the performance of solar chimneys. If the water is hot compared to the air, heat is transferred from the water to the air, raising its temperature. This improves the updraft in the chimney. For cold water, it decreases the air temperature. This raises the density of the air, which improves the natural downdraft in the chimney, which is useful for a U-tube chimney; in that case, pumping power is required to spray the water at the outlet of the chimney. Some hybrid systems with cooling pond systems may also provide this benefit.

Over the past few years, various scientists have put forth geoengineering initiatives centered around solar chimneys, and numerous researchers have constructed prototypes aimed at addressing the issue of haze and enhancing urban air quality. Table 6 provides a concise overview of these endeavors.

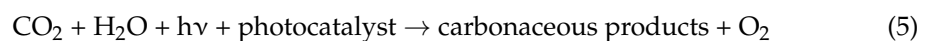
Table 6. Overview of mitigation strategies.

Source	Techniques	Location Considered
Zhou et al. [72]	No-filter, large-height (1 to 1.5 km) solar chimney	China, Beijing
Cao et al. [71]	With and without filter	-
Tan et al. [161]	Filter-containing urban updraft tower (FUUT)	China, Beijing
Cao et al. [162]	Filter	Xi'an, China
Ghanbari and Rezazadeh [163]	No filter, effect of the tower	City of Tehran
Daghistani [164]	No filter, only the effect of the street pole	Riyadh, Saudi Arabia
Hachicha et al. [165]	Filter and its location	Case study in Sharjah
Yoo et al. [166]	Filter's impact on power generation and air cleaning	-
Gong et al. [167]	Filter, cooling tower, and water spray	-

4. Case Studies of SCPPs for Air Pollution Mitigation

CO₂ is a major contributor to global warming and accounts for a 65% share of the total well-mixed long-lived GHGs [168]. To reduce the concentration of carbon dioxide and thus slow down global warming, several innovative solutions like Carbon Capture and Storage (CCS), Bioenergy with Carbon Capture and Storage (BECCS), and Direct air capture (DAC) were developed by scientists. De_Richter et al. [113] first proposed the idea of hybridization of SCPPs with a giant photocatalytic reactor for artificial photosynthesis by semiconductor photocatalysis. The photocatalytic conversion of CO₂ not only reduces the concentration of CO₂ but also produces fuels in a continuous-flow photocatalytic reactor with natural sunlight.

The photocatalytic reduction of carbon dioxide occurs according to the following reaction:



Several photocatalysts and methods were used by researchers for the photoreduction of carbon dioxide. The most common catalyst is TiO₂ and its derivatives. The products of the reaction are generally methane or methanol with other products [119,169–173]. The yield and product distribution depend on the photocatalyst that is used and the reaction conditions. The best yield is obtained after 6 to 24 h of illumination in batch reactors. This implementation of the process requires a photoreactor. Mostly, three types of photocatalytic reactors are available, plate, honeycomb, and tubular [174].

Figures 5 and 6 show the two possible implementations of hybrid SCPPs proposed by de-Richter et al. [113]. This choice depends upon the process parameters and, of course, the photocatalyst that is used. The up-scaling to the size of an SCPP assumes that the photocatalytic conversion of CO₂ occurs only once. They reported that 1.938 mol of carbon dioxide (85 gm) can be reduced per gm of catalyst per year if two cycles of 6 h can be operated every day throughout the year. If 3452 tons of CO₂ can be captured daily by the solar tower, 737 tons of catalyst is theoretically needed to convert 5% of the captured CO₂ to fuel every day.

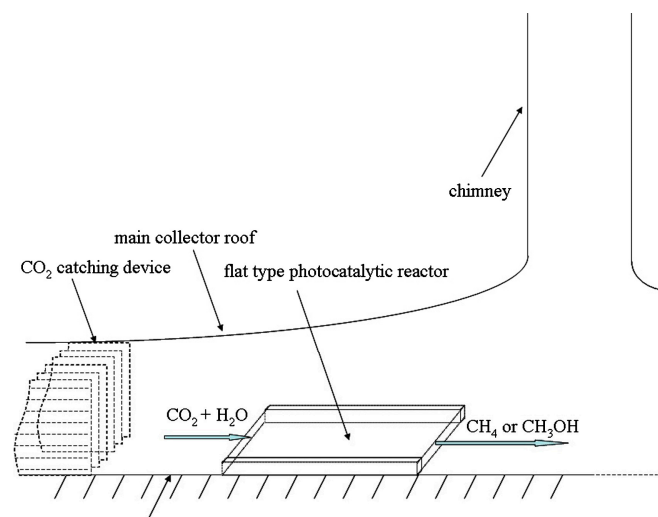


Figure 5. Location of flat photocatalytic reactor in SCPP (inside translucent photocatalyst), de-Richter et al. [113].

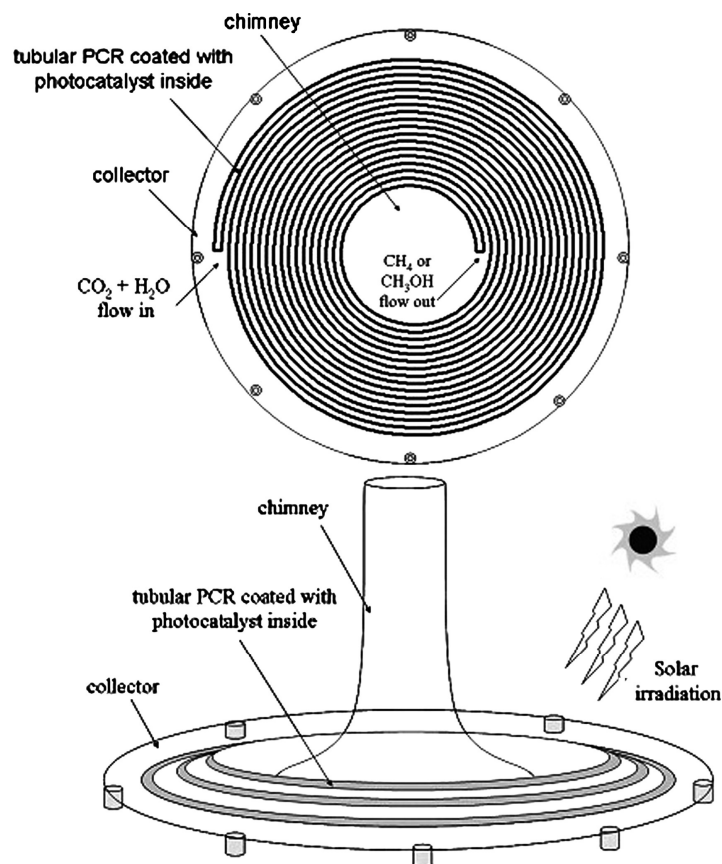


Figure 6. Top view and side view of tubular photocatalytic reactor (inside translucent photocatalyst), de-Richter et al. [113].

Although CO_2 is the main GHG, it is not possible to slow down global warming by only controlling CO_2 . It can be seen from Table 7 that GWPs of CH_4 are 28 times more potent than that of CO_2 over 100 time periods, which means that 1 kg of methane emitted today would exert 28 times as much global warming over the next 100 years as 1 kg of CO_2 emitted today would. Similarly, the warming effect of 1 kg of N_2O emitted today would

be the same as 298 kg of CO₂ released today over the next 100 years. Thus, the removal of non-CO₂ GHGs is also necessary to mitigate climate change.

Table 7. Concentrations and GWP of major GHGs as per IPCC (IPCC_AR5 2013) [14].

GHG Type	Concentrations in 2011	Radiative Forcing in 2011 (W/m ²)	*GWP (100-Year Time Horizon)	Atmospheric Life Time (Years)
Carbon dioxide	391 ± 0.2 ppm	1.82 ± 0.19	1	100–300
Methane	1803 ± 2 ppb	0.48 ± 0.05	28	12
Nitrous oxide	324 ± 0.1 ppb	0.17 ± 0.03	298	121

*GWP is the measure of global warming potential.

Ming et al. [175] proposed a combination of SCPP-PCR to efficiently remove N₂O, one of the important GHGs, from the atmosphere. This proposal was an extension of the idea introduced by de-Richner et al. (2013) [113] for the catalytic conversion of atmospheric CO₂. de Richter et al. [114] introduced a hybrid SCPP-PCR that will eliminate GHGs in addition to producing renewable energy. They also mentioned that the effectiveness of this new technology at an ambient temperature and relative humidity depends on the fulfillment of the following conditions:

- The presence of an efficient visible-light photocatalyst for effective conversion of non-carbon dioxide greenhouse gases.
- Higher solar radiation for several hours for the activation of the photocatalyst.
- A higher and continuous air flux bringing the irradiated photocatalyst in touch with polluted air containing non-CO₂ GHGs, like nitrous oxide, methane, and halocarbons.

Here, an SCPP appears to be a good candidate to fulfill the above criteria, as it has the following characteristics:

- A very large solar collector for a higher GH (green house) effect that gives a wide illuminated area for a photocatalytic reaction.
- A large chimney for a better draft.
- A provision for a thermal energy storage layer below the absorber to store energy for nighttime operation.

Finally, an SCPP contains severable turbines which generate decarbonized renewable energy. For a 200 MW SCPP, the area of the GH collector is 38 km², the volume of airflow through the collector is 17 km³/day, and the amount of solar radiation that is received is >2200 kW m⁻² year⁻¹. Then, with the current atmospheric concentration, this SCPP air flow will contain 7900 tons of methane, 3900 tons of nitrous oxide, and nearly 42 tons of halogenated compounds. Figures 7 and 8 show the proposed configurations of the SCPP-PCR. In the SCPP, the air flow direction is constant, and it occurs radially towards the collector center. In Figure 7, the best direction of solar radiation is mostly maintained. The presence of partition walls prevents the disturbance from external rapid crosswinds and maintains the slow flow of hot air below the GH. The partition walls also guide the movement of the ambient crosswind passing below the GH by the front compartment and toward the air turbines, located near the chimney base. The inner side of the glass collector of the SCPP is covered with translucent photocatalysts. The ground under the GH collector is also equipped with another type of photocatalyst. In Figure 7, multiple translucent layers of photocatalysts are suggested at the entry to the SCPP for maximizing the contact hours between the GHGs that are present in the inlet air and the photocatalyst coating. The use of multiple layers improves the surface volume and mass transfer, but the intensity of the visible light decreases progressively at the same time for multiple layers of coated glass or polymeric sheets. Moreover, in Figure 7, a very large photocatalyst area may allow for a longer contact time and photocatalyst illumination, but the rate of mass transfer can be poorer due to thicker boundary layers.

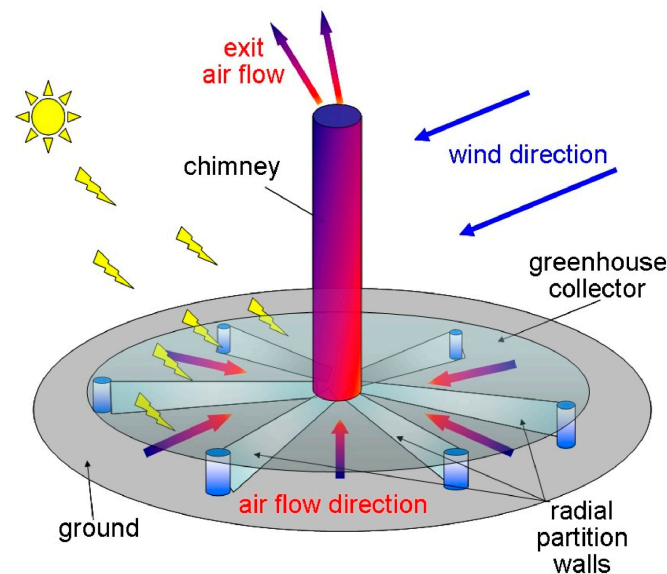


Figure 7. Positions of translucent photocatalyst inside glass canopy of SCPP [114].

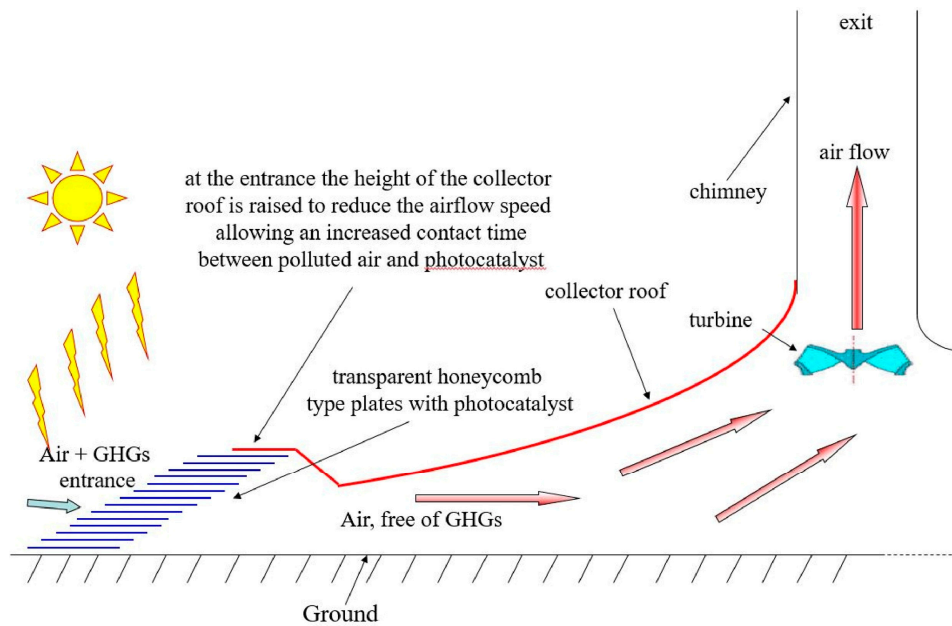


Figure 8. Multiple layers of photocatalysts installed under the GH around the circumference of the SCPP [114].

Roughly, one atmospheric volume could undergo purification over a span of 15 years as it passes through SCPPs, assuming the installation of 50,000 SCPPs. These plants, each with a capacity of 200 MW or 680 GWh at a 39% capacity factor, could potentially meet the anticipated future energy demand of 10,000 GW under the given assumptions.

Ming et al. [176] investigated the performance and influencing factors of photocatalytic oxidation of methane by the SCPP-PCR system (Figure 9). They used the CFD model for their study. They selected a honeycomb monolith photoreactor to design a PCR, and the internal channel surface of the honeycomb monolith PCR was assumed to be coated with TiO_2 . The geometry of the SCPP was the same as the original SCPP built in Manzanares. The result revealed that 21.312 kg of methane can be degraded per day with this SCPP-PCR system under the solar radiation conditions of Qianyanzhou, China, when the channel diameter of the PCR is set at 4 mm and the channel length is 8 m.

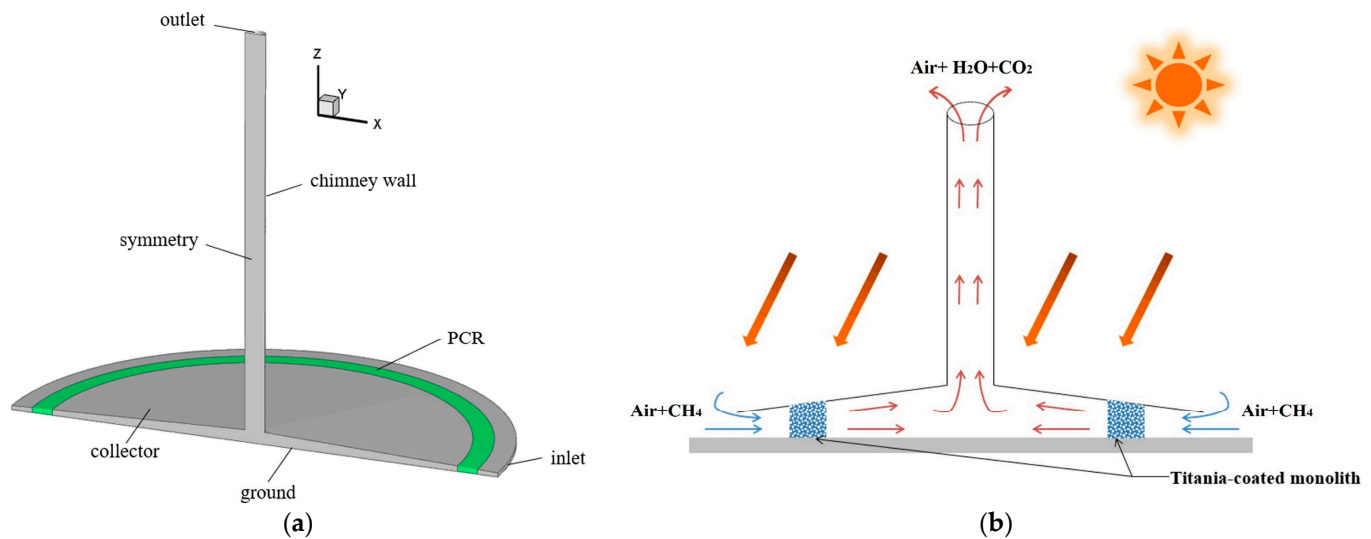


Figure 9. Overview of SCPP-PCR system with different components of SCPP [176], (a) three-dimensional view, and (b) two-dimensional view.

Recently, Xiong et al. [177] carried out a comprehensive numerical analysis to study the potential of an SCPP-PCR for methane removal. The study revealed that an SCPP integrated with an HPCR (honeycomb photocatalytic reactor) exhibits better performance compared to a PPCR (flat photocatalytic reactor) for the degradation of atmospheric methane under ambient crosswind. When the velocity of the ambient crosswind (ACW) = 0 m/s, the rate of degradation of methane with an SCPP-PPCR is 0.89 g/s, and with an SCPP-HPCR, it is 0.54 g/s. But with the increase in the flow rate of the ambient crosswind, the rate of degradation of methane with an SCPP-PPCR decreases quickly and then stabilizes at 0.11 g/s, whereas with an SCPP-HPCR, the rate of degradation of methane stabilizes at 0.41 g/s.

The integration of an SCPP with a PCR not only addresses environmental issues like global warming and ozone layer depletion but also provides a sustainable solution to the global energy crisis. From an economic point of view, a hybrid SCPP-PCR system is also advantageous.

As the SCPP infrastructure provides the support for the PCR, the installation of a hybrid SCPP-PCR requires a minimum additional investment. With the following assumptions, the amount of photocatalysts needed to build up the hybrid system would be 1000 tons (as the density of TiO_2 is approximately 3900 kg per m^3).

- Nano- TiO_2 will be used as a photocatalyst.
- Photocatalysts will be applied at the center of the GH collector, and a radius of 2.5 km will be covered with the photocatalysts.
- A single layer of coating contains 50 g per m^2 of nano-sized TiO_2 .

Considering the price of bulk nano-sized TiO_2 of 3300 USD per ton, the cost of 1000 tons of nano-sized TiO_2 would be around USD 3–4 million. The overall estimated cost of the coating process would be USD 20 million, which is less than 2% of the cost of the SCPP [114].

Apart from this, atmospheric clean-up by the successful implementation of an SCPP-PCR system can provide a benefit that is comparable to that of the Montreal Protocol [178].

An SCPP with a filter for both electricity and cleaning the air was studied numerically by Hachicha et al. [165]. The research utilized the geometric dimensions of Manzanares as a basis for their investigation. The schematic diagram with the filter is shown in Figure 10. Multi-objective optimization to find the correct filter location and maximize the power is carried out at different locations by using response surface methodology. The connection of the filter is established at both the inlet of the collector and the inlet of the chimney. The filter locations at the collector entry show better performance. The power output for

the hybrid system is 8.3 kW, and the flow rate of clean air is 447 m³/s. They revealed that the reduction in power is 6% because of the filter addition.

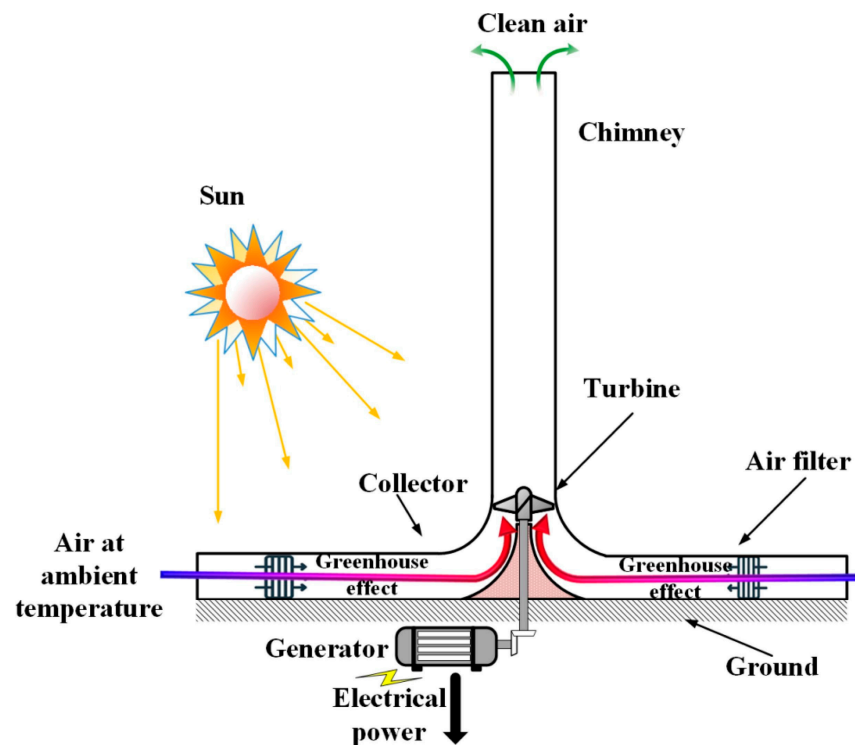


Figure 10. Schematic diagram of SCPP with filter [165].

Cao et al. [71] presented numerical findings on a Solar-Assisted Large-Scale Cleaning System (SALSCS) with a height of 500 m. The system is designed to effectively segregate PM_{2.5} and larger particulate matter using a filter bank. The numerical analysis incorporated a substantial collector area, featuring a radius dimension of 2500 m. A fluid flow and heat transfer study was carried out with and without filter. The use of a filter decreases the airflow velocity but raises the overall system's pressure drop and temperature. They set a requirement that their system should be able to clean air of 2.64×10^5 m³/s. Furthermore, Cao et al. [165] investigated, both experimentally and numerically (in Xi'an, China), a system with 60 chimney and solar collectors of 43×60 m² and showed a 73.5% filter efficiency for PM_{2.5}.

In their 2015 study, Zhou et al. [72] employed a solar updraft tower with heights of 1 km and 1.5 km, excluding a collector, to redirect haze-laden air to higher altitudes. The collector effect is induced by an urban heat island (UHI), and this facility can generate electrical power on days with lower pollution levels. Their study was related to the study considering the environment in Chinese cities. Apart from the performance study, a cost analysis of the updraft tower was included in their investigation. Using air in an urban heat island (UUI), Tan et al. [161] proposed a filter-based urban updraft tower to produce power as well as electricity. The filter is mainly for removal of air pollution of particulate matter up to PM_{2.5}, considering metropolitan cities in China, such as Beijing in 2012. The UHI effect is observed more in metropolitan cities at day and night. The dimensions of the chimney are, as per Zhou et al. [72], a chimney height of 1 km and a diameter of 0.11 m. The researchers analyzed the plant's performance and assessed the associated health- and economic benefits. Their findings demonstrate that the plant has the potential to achieve a reduction of 6.72 µg/m³ in the first year.

Daghistani [164] repurposed a streetlight pole as a solar chimney to eliminate air pollutants near the street surface. This innovative system offers the advantage of not requiring additional space for implementation, providing cleaner air for pedestrians. In this

setup, solar energy heats the air through the wall. The pole has a large hole at the bottom for air entry. Some small holes with transparent covers are distributed at the walls to transfer solar energy for a convective flow of the air. Therefore, the passive movement of polluted air due to a buoyancy force goes upward through the pole to a higher elevation. A solar panel is fixed at the top of the pole for streetlights. At night or in low-sunlight conditions, the photovoltaic cell powers an exhaust fan that is fitted at the top to generate the active flow of air through the pole. The proposed pole is shown in Figure 11. The numerical work shows an updraft air magnitude of $6.97 \text{ m}^3/\text{min}$ on a summer day in Riyadh, Saudi Arabia.

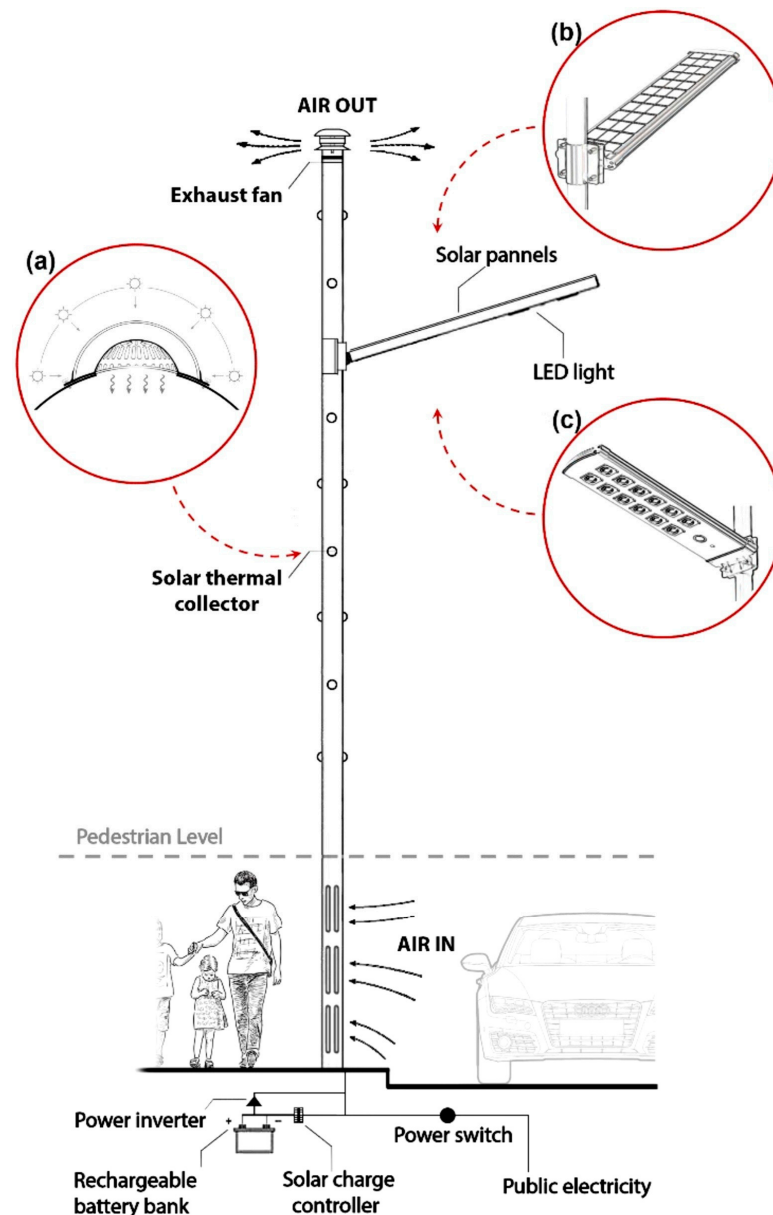


Figure 11. View of street light pole acting as a solar chimney [164].

Yoo et al. [166] conducted a numerical study on a hybrid system combining an SCPP and an SALSCS, commonly referred to as filter-equipped SCPP (FSCPP). The simulations utilized the dimensions from the Manzanares plant. In addition to investigating the fluid flow and heat transfer, the study involved a comprehensive performance comparison among SCPPs, SALSCSs, and FSCPPs, with a detailed focus on numerical methods. Notably, the filter in the FSCPP was positioned at the chimney entry. The results revealed a 20–40%

power reduction for the FSCPP compared to the SCPP alone, while the air purification in the FSCPP exhibited a 2–4% reduction compared to the SASLCS.

In their 2019 study, Ghanbari and Rezaadeh [163] employed solar chimneys ranging from 100 to 300 m in length, with a diameter of 40 m, for dispersing polluted air in urban areas. Their numerical investigation specifically examined how the atmospheric conditions influence the ventilation efficiency of the chimney. The findings indicate that the chimney performs more effectively in unstable conditions and at lower ambient temperatures. Moreover, the study highlights superior performance in cities that are situated near the sea level, exemplified by the city of Tehran.

In their 2017 study, Gong et al. [167] advocated for the adoption of an inverted U-type cooling tower, depicted in their work (Figure 12), as a solution focused on mitigating air pollution rather than generating power. In their numerical work, they considered the impact of filters, cooling towers, and water sprays on controlling clean air. The basic dimensions of the solar chimney were taken from the Manzanares plant. A filter is attached at the collector entry to filter $PM_{2.5}$ and other particles, and a water-spraying system is connected in the bending of the U-tube for evaporative cooling. The air becomes heavier and falls automatically because of the downdraft, and clean air goes to the atmosphere and improves the quality of the air. According to their research, the facility generates purified air with a volumetric flow rate of $810 \text{ m}^3/\text{s}$.

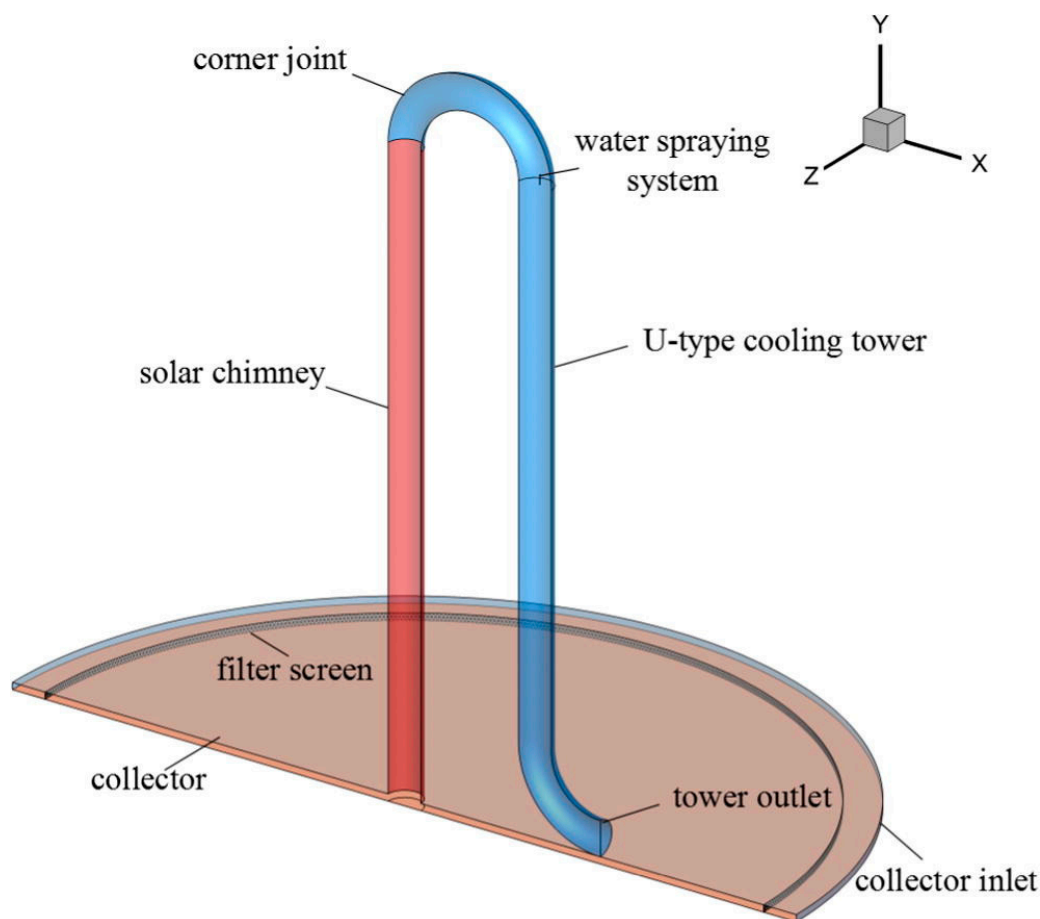


Figure 12. Incorporation of water spraying system in U-type cooling tower [167].

The summary of the above case studies for the removal of PM as well as greenhouse gases is tabulated in Table 8.

Table 8. A summary of different case studies for the removal of PM as well as greenhouse gases.

Authors	Type of Study	Photocatalyst Used	Key Controlling Parameters	Gas/PM/Air Removal	Results
de-Richter et al. [113]	Theoretical	TiO ₂	Premature stage. Difficult to identify key controlling parameters. Of course, selection of catalyst is important.	Carbon dioxide	Mitigation of atmospheric CO ₂ concentration. Generation of fuels and/or value-added chemicals. Simultaneous production of carbon-free renewable electricity.
Ming et al. [175]	Theoretical	(i) Translucent thin film of metal-doped TiO ₂ on solar chimney glass (ii) Metal-exchanged zeolites at base of solar chimney	(i) Natural sunlight irradiation (>2000 kw/m ² /year). (ii) Continuous air flow under solar chimney. (iii) Ambient temperature of hot arid climate countries.	N ₂ O	Transformation of N ₂ O to N ₂ and O ₂ , which are harmless for ozone layer. Simultaneous generation of carbon-free renewable electricity.
de Richter et al. [114]	Theoretical	TiO ₂	(i) Type of reactor (PPCR or HPCR). (ii) Location of photocatalyst under SCPP. (ii) Light availability and penetration to photocatalyst.	CH ₄ , N ₂ O, Halocarbons	Removal of atmospheric non-CO ₂ GHGs can provide benefit which is equivalent to removal of 1600 ktons of CO ₂ per year. Requires minimum additional investment for integration with PCR.
Ming et al. [176]	Numerical	TiO ₂	Pore diameter and channel length of honeycomb monolith photocatalytic reactor.		Integration of SCPP with PCR can degrade 21.3 kg methane per day under intense sunlight (10 h/day) such as in Qianyanzhou, China, provided pore diameter and length of PCR are 4 mm and 8 m, respectively.
Xiong et al. [177]	Numerical	P-25	(i) Choice of reactor (PPCR or HPCR). (ii) Velocity of ambient crosswind (ACW).		Photodegradation rate of methane depends on flow rate of ambient crosswind. Performance of SCPP-HPCR is better compared to SCPP-PPCR under strong ambient crosswind conditions.

Table 8. Cont.

Authors	Type of Study	Photocatalyst Used	Key Controlling Parameters	Gas/PM/Air Removal	Results
Hachicha et al. [165]	Numerical -		Filter.	PM	<ul style="list-style-type: none"> • Perfect filter locations are at collector entry. • 6% reduction in power because of used filter.
Cao et al. [71]	Numerical -		Filter.	PM _{2.5}	<ul style="list-style-type: none"> • Filter addition decreases airflow velocity but raises overall system pressure drop and temperature.
Cao et al. [162]	Numerical/Experimental		Filter.	PM _{2.5}	<ul style="list-style-type: none"> • Predicts 73.5% filter efficiency for PM_{2.5}.
Zhou et al. [72]	Numerical -		Air dispersion by solar updraft tower.	Air	<ul style="list-style-type: none"> • Cost analysis is carried out. • Reduction in pollutants is 6.72 µg/m³ in first year.
Tan et al. [161]	Numerical -		Filter.	PM ₁₀	<ul style="list-style-type: none"> • Proposed reduction is 6.72 µg/m³ in first year. • Conducted economic capability analyses.
Daghistani [164]	Numerical -		Streetlight as chimney.	Air	<ul style="list-style-type: none"> • Street light is used as solar chimney. • Updraft air magnitude of 6.97 m³/min in one day.
Yoo et al. [166]	Numerical -		Filter.	PM	<ul style="list-style-type: none"> • Reduction in power is 20–40% due to the filter.
Ghanbari and Rezazadeh [163]	Numerical -		Air dispersion by chimney.	Air	<ul style="list-style-type: none"> • Chimney performs more effectively in unstable conditions and at lower ambient temperatures.
Gong et al. [167]	Numerical -		Filter.	PM _{2.5}	<ul style="list-style-type: none"> • Generates purified air with volumetric flow rate of 810 m³/s.

5. Conclusions and Recommendations

In conclusion, this comprehensive review underscores the multifunctional potential of Solar Chimney Power Plants (SCPPs) in tackling urban air pollution. The prescribed strategies, including elevation mechanisms, filter integration, and photocatalytic reactors, present versatile solutions for addressing both particulate matter and greenhouse gases. The integration of photocatalytic reactors (PCRs) proves to be superior in methane degradation, showcasing promising results for GHG removal. Case studies, ranging from filter-equipped SCPPs to innovative Solar-Assisted Large-Scale Cleaning Systems (SALSCSs), demonstrate the versatility of SCPP applications in real-world scenarios. The challenges associated with filter integration and optimizations for power generation and air purification are meticulously evaluated, providing valuable insights for future research. Furthermore, recent geoengineering actions based on solar chimneys open new avenues for urban air quality management.

This review serves as a foundational resource, emphasizing the urgency of adopting holistic approaches to combat air pollution while harnessing renewable energy sources. As we stand at the intersection of technological innovation and environmental stewardship, SCPPs emerge as promising tools for sustainable urban development, cleaner air, and a healthier planet.

Concluding with a synthesis of insights, this review serves as a guide for researchers and policymakers, emphasizing the need for multifaceted approaches to address the intricate nexus of air pollution, renewable energy generation, and climate change mitigation.

In conclusion, this study holds economic and social importance through its ability to promote the cost-effective generation of clean energy, spur job creation, enhance public health, broaden access to sustainable energy, and play a role in global initiatives aimed at mitigating climate change.

This assures the researchers of better utilization of a plant after geometry modification and hybridization. All types of utilizations in combination may improve the performance of a plant. This will guide the researchers in such practical endeavors.

Author Contributions: Conceptualization: D.K.M. and S.B.; methodology: N.B.; software: D.K.M.; validation: N.K.M.; formal analysis: D.K.M. and S.B.; investigation: N.B. and E.C.; resources: S.B.; data curation: D.K.M. and S.B.; writing—original draft preparation: D.K.M. and S.B.; writing—review and editing: D.K.M. and N.B.; visualization: N.K.M.; supervision: E.C.; review: A.C.B.; supervision and project administration: A.C.B. All authors have read and agreed to the published version of the manuscript.

Funding: This research received no external funding.

Institutional Review Board Statement: Not applicable.

Informed Consent Statement: Not applicable.

Data Availability Statement: Not applicable.

Conflicts of Interest: The authors declare no conflict of interest.

References

1. WHO. Air Pollution, The Invisible Health Treat. 2023. Available online: <https://www.who.int/news-room/feature-stories/detail/air-pollution--the-invisible-health-threat> (accessed on 15 December 2023).
2. WHO. Ambient (Outdoor) Air Pollution. 2022. Available online: [https://www.who.int/news-room/fact-sheets/detail/ambient-\(outdoor\)-air-quality-and-health](https://www.who.int/news-room/fact-sheets/detail/ambient-(outdoor)-air-quality-and-health) (accessed on 16 December 2023).
3. Ramanathan, V.; Feng, Y. Air Pollution; Greenhouse gases and climate change, global and regional perspectives. *Atmos. Environ.* **2009**, *43*, 37–50. [[CrossRef](#)]
4. Pöschl, U. Atmospheric Aerosols, Composition, Transformation; Climate and Health Effects. *Angew. Chem. Int. Ed.* **2005**, *44*, 7520–7540. [[CrossRef](#)]
5. Li, Z.; Yu, S.; Wang, L.; Mehmood, K.; Liu, W.; Alapaty, K. Suppression of convective precipitation by elevated man-made aerosols is responsible for large-scale droughts in north China. *Proc. Natl. Acad. Sci. USA* **2018**, *115*, E8327. [[CrossRef](#)]

6. Yu, S.; Li, P.; Wang, L.; Wang, P.; Wang, S.; Chang, S.; Liu, W.; Alapaty, K. Anthropogenic aerosols are a potential cause for migration of the summer monsoon rain belt in China. *Proc. Natl. Acad. Sci. USA* **2016**, *112*, E2209. [CrossRef]
7. US EPA. Basic Information about Visibility. 2020. Available online: <https://www.epa.gov/visibility/basic-information-about-visibility> (accessed on 13 March 2020).
8. Wu, D.; Bi, X.; Deng, X.; Li, F.; Tan, H.; Liao, G.; Huang, J. Effect of atmospheric haze on the deterioration of visibility over the Pearl River Delta. *Acta Meteorol. Sin.* **2007**, *21*, 215–223.
9. Battisti, L. Energy power and greenhouse gas emissions for future transition scenarios. *Energy Policy* **2023**, *179*, 113626. [CrossRef]
10. Nd Energiewende and Ember; The European Power Sector in 2020, Up-to-Date Analysis of the Electricity Transition; Version 1.0. AEE. 202/02-a-2021/EN. 2021. Available online: <https://www.iea.org/reports/net-zero-by-2050> (accessed on 15 January 2024).
11. Blakers, A.; Mathiesen, B.V.; Breyer, C.; Weber, E.; Fell, H.-J.; Jacobson, M.Z.; Seba, T. Joint Declaration of the Global 100% Renewable Energy Strategy Group. 2021. Available online: <https://global100restrategygroup.org/> (accessed on 15 January 2024).
12. REN21. Renewables 2021 Global Status Report. Paris. 2021. Available online: <https://www.ren21.net/reports/global-status-report> (accessed on 15 January 2024).
13. Masters, G.M. *Introduction to Environmental Engineering and Science*, 2nd ed.; Prentice-Hall of India: New Delhi, India, 2005.
14. IPCC_AR5 2013. Available online: <https://www.ipcc.ch/report/ar5/syr/> (accessed on 24 May 2015).
15. Romanello, M.; McGushin, A.; Napoli, C.D.; Drummond, P.; Hughes, N.; Jamart, L.; Kennard, H.; Lampard, P.; Rodriguez, B.S.; Arnell, N. The 2021 report of the Lancet Countdown on health and climate change, code red for a healthy future. *Lancet* **2021**, *398*, 1619–1662. [CrossRef] [PubMed]
16. Portner, H.-O.; Roberts, D.C.; Poloczanska, E.S.; Mintenbeck, K.; Tignor, M.; Alegría, A.; Craig, M.; Langsdorf, S.; Loschke, S.; Moller, V. Summary for Policymakers. Climate Change 2022-Impacts. In *Adaptation and Vulnerability, Working Group II Contribution to the Sixth Assessment Report of the Intergovernmental Panel on Climate Change*; Cambridge University Press: Cambridge, UK; UNEP: Nairobi, Kenya, 2022.
17. Chen, Z.; Zhou, T.; Zhang, L.; Chen, X.; Zhang, W.; Jiang, J. Global land monsoon precipitation changes in CMIP6 projections. *Geophys. Res. Lett.* **2020**, *47*, e2019GL086902. [CrossRef]
18. Hirabayashi, Y.; Mahendran, R.; Koirala, S.; Konoshima, L.; Yamazaki, D.; Watanabe, S.; Kim, H.; Kanae, S. Global flood risk under climate change. *Nat. Clim. Chang.* **2013**, *3*, 816–821. [CrossRef]
19. Stocker, T.F.; Qin, D.; Plattner, G.-K.; Tignor, M.; Allen, S.K.; Boschung, J.; Nauels, A.; Xia, Y.; Bex, V.; Midgley, P.M. (Eds.) Climate Change 2013. In *The Physical Science Basis Contribution of Working Group I to the Fifth Assessment Report of the Intergovernmental Panel on Climate Change*; Cambridge University Press: Cambridge, UK; New York, NY, USA, 2013; pp. 1029–1136.
20. Deng, S.Z.; Jalaludin, B.B.; Anto, J.M.; Hess, J.J.; Huang, C.R. Climate change; air pollution; and allergic respiratory diseases, a call to action for health professions. *Chin. Med. J.* **2020**, *133*, 1552–1560. [CrossRef] [PubMed]
21. Jin, X.; Ren, J.; Li, R.; Gao, Y.; Zhang, H.; Li, J.; Zhang, J.; Wang, X.; Wang, G. Global burden of upper respiratory infections in 204 countries and territories; from 1990 to 2019. *EclinicalMedicine* **2021**, *37*, 100986. [CrossRef]
22. Yao, M.; Hu, Y.; Zhang, A.; Ji, J.S.; Zhao, B. COPD deaths attributable to ozone in 2019 and future projections using the WHO AQG 2021 in urban China. *Eco-Environ. Health* **2022**, *1*, 251–258. [CrossRef]
23. Zhao, Q.; Yu, P.; Mahendran, R.; Huang, W.; Gao, Y.; Yang, Z.; Ye, T.; Wen, B.; Wu, Y.; Li, S.; et al. Global climate change and human health, Pathways and possible solutions. *Eco-Environ. Health* **2022**, *1*, 53–62. [CrossRef]
24. Hu, S.; Fruin, S.; Kozawa, K.; Mara, S.; Paulson, S.E.; Winer, A.M. A wide area of air pollutant impact downwind of a freeway during pre-sunrise hours. *Atmos. Environ.* **2009**, *43*, 2541–2549. [CrossRef]
25. Zhu, Y.; Kuhn, T.; Mayo, P.; Hinds, W.C. Comparison of daytime and nighttime concentration profiles and size distributions of ultrafine particles near a major highway. *Environ. Sci. Technol.* **2006**, *40*, 2531–2536. [CrossRef]
26. Quiros, D.C.; Lee, E.S.; Wang, R.; Zhu, Y. Ultrafine particle exposures while walking; cycling; and driving along an urban residential roadway. *Atmos. Environ.* **2013**, *73*, 185–194. [CrossRef]
27. Edussuriya, P.; Chan, A.; Ye, A. Urban morphology and air quality in dense residential environments in Hong Kong. Part I, District-level analysis. *Atmos. Environ.* **2011**, *45*, 4789–4803. [CrossRef]
28. Zhang, J.; Li, Y.; Tao, W.; Liu, J.; Levinson, R.; Mohegh, A.; Ban-Weiss, G. Investigating the urban air quality effects of cool walls and cool roofs in Southern California. *Environ. Sci. Technol.* **2019**, *53*, 7532–7542. [CrossRef] [PubMed]
29. Grimm, N.B.; Faeth, S.H.; Golubiewski, N.E.; Redman, C.L.; Wu, J.; Bai, X.; Briggs, J.M. Global change and the ecology of cities. *Science* **2008**, *319*, 756–760. [CrossRef] [PubMed]
30. Epstein, S.A.; Lee, S.-M.; Katzenstein, A.S.; Carreras-Sospedra, M.; Zhang, X.; Farina, S.C.; Vahmani, P.; Fine, P.M.; Ban-Weiss, G. Air-quality implications of widespread adoption of cool roofs on ozone and particulate matter in southern California. *Proceed. Natl. Acad. Sci. USA* **2017**, *114*, 8991–8996. [CrossRef] [PubMed]
31. Caiazzo, F.; Ashok, A.; Waitz, I.A.; Yim, S.H.L.; Barrett, S.R.H. Air pollution and early deaths in the United States. Part I, Quantifying the impact of major sectors in 2005. *Atmos. Environ.* **2013**, *79*, 198–208. [CrossRef]
32. Cohen, A.J.; Brauer, M.; Burnett, R.; Anderson, H.R.; Frostad, J.; Estep, K.; Balakrishnan, K.; Brunekreef, B.; Dandona, L.; Dandona, R.; et al. Estimates and 25-year trends of the global burden of disease attributable to ambient air pollution, an analysis of data from the Global Burden of Diseases Study 2015. *Lancet* **2017**, *389*, 1907–1918. [CrossRef]
33. Tsai, S.S.; Chiu, Y.W.; Weng, Y.H.; Yang, C.Y. Association between fine particulate air pollution and the risk of death from lung cancer in Taiwan. *J. Toxicol. Environ. Health A* **2022**, *85*, 431–438. [CrossRef]

34. Boogaard, H.; Patton, A.P.; Atkinson, R.W.; Brook, J.R.; Chang, H.H.; Crouse, D.L.; Fussell, J.C.; Hoek, G.; Hoffmann, B.; Kappeler, R.; et al. Long-term exposure to traffic-related air pollution and selected health outcomes, a systematic review and meta-analysis. *Environ. Int.* **2022**, *164*, 107262. [CrossRef]
35. Chung, C.Y.; Yang, J.; Yang, X.; He, J. Long term effects of ambient air pollution on lung cancer and COPD mortalities in China, a systematic review and meta analysis of cohort studies. *Environ. Impact Assess. Rev.* **2022**, *97*, 106865. [CrossRef]
36. Kumar, M. Global, regional, and national comparative risk assessment of 84 behavioural, environmental and occupational, and metabolic risks or clusters of risks for 195 countries and territories, 1990–2017, a systematic analysis for the Global Burden of Disease Study 2017. *Lancet* **2018**, *392*, 1923–1994.
37. Gao, Y.; Ji, H. Microscopic morphology and seasonal variation of health effect arising from heavy metals in PM_{2.5} and PM₁₀, One-year measurement in a densely populated area of urban Beijing. *Atmos. Res.* **2018**, *212*, 213–226. [CrossRef]
38. Jose, S.; Gharai, B.; Kumar, Y.; Venkata, P.; Rao, N. Radiative implication of a haze event over Eastern India. *Atmos. Pollut. Res.* **2015**, *6*, 138–146. [CrossRef]
39. Lin, Y.; Zou, J.; Yang, W.; Li, C.-Q. A Review of Recent Advances in Research on PM_{2.5} in China. *Int. J. Environ. Res. Public Health* **2018**, *15*, 438. [CrossRef] [PubMed]
40. Sulong, N.A.; Latif, M.T.; Khan, M.F.; Amil, N.; Ashfold, M.J.; Wahab, M.I.A.; Chan, K.M.; Sahani, M. Source apportionment and health risk assessment among specific age groups during haze and non-haze episodes in Kuala Lumpur, Malaysia. *Sci. Total Environ.* **2017**, *601–602*, 556–570. [CrossRef] [PubMed]
41. WHO Global Air Quality Guidelines, Particulate Matter (PM_{2.5} and PM₁₀) Ozone, Nitrogen Dioxide, Sulfur Dioxide and Carbon Monoxide. Available online: <https://www.who.int> (accessed on 22 September 2021).
42. Zhou, X.; Wang, F.; Ochieng, R.M. A review of solar chimney power technology. *Renew. Sustain. Energy Rev.* **2010**, *14*, 2315–2338. [CrossRef]
43. Dhahri, A.; Omri, A. A Review of solar chimney power generation technology. *Int. J. Eng. Adv. Technol.* **2013**, *2*, 1–17.
44. Bais, R.; Saxena, N.V. A review on solar chimney power plant performance. *Int. J. Sci. Eng. Dev. Res.* **2021**, *6*, 32–37.
45. Cuce, E.; Cuce, P.M.; Carlucci, S.; Sen, H.; Sudhakar, K.; Hasanuzzaman, M.; Daneshazarian, R. Solar chimney power plants, a review of the concepts; designs and performances. *Sustainability* **2022**, *14*, 1450. [CrossRef]
46. Bansod, P.J.; Thakre, S.B.; Wankhade, N.A. Solar chimney power plant—a review. *Int. J. Mod. Eng. Res.* **2014**, *4*, 18–33.
47. Pradhan, S.; Chakraborty, R.; Mandal, D.K.; Barman, A.; Bose, P. Design and performance analysis of solar chimney power plant (SCPP): A Review. *Sustain. Energy Technol. Assess.* **2021**, *47*, 101411. [CrossRef]
48. Guo, P.; Li, T.; Xu, B.; Xu, X.; Li, J. Questions and current understanding about solar chimney power plant: A review. *Energy Conv. Manag.* **2019**, *182*, 21–33. [CrossRef]
49. Al-Kayiem, H.H.; Aja, O.C. Historic and recent progress in solar chimney power plant enhancing technologies. *Renew. Sustain. Energy Rev.* **2016**, *58*, 1269–1292. [CrossRef]
50. Bayarrah, M. Exergy analysis of solar chimney power plants, a review. *Sustain. Energy Technol. Assess.* **2022**, *53*, 102568. [CrossRef]
51. Ahmed, O.K.; Algburi, S.; Ali, Z.H.; Ahmed, A.K.; Shubat, H.N. Hybrid solar chimneys: A comprehensive review. *Energy Rep.* **2022**, *8*, 438–460. [CrossRef]
52. Das, P.; Chandramohan, V.P. A review on recent advances in hybrid solar updraft tower plants, Challenges and future aspects. *Sustain. Energy Technol. Assess.* **2023**, *55*, 102978. [CrossRef]
53. Chikere, A.O.; Al-Kayiem, H.H.; Karim, Z.A.A. Review on the enhancement techniques and introduction of an alternate enhancement technique of solar chimney power plant. *J. Appl. Sci.* **2011**, *11*, 1877–1884. [CrossRef]
54. Biswas, N.; Mandal, D.K.; Bose, S.; Manna, N.K.; Benim, A.C. Experimental treatment of solar chimney power plant—A comprehensive review. *Energies* **2023**, *16*, 6134. [CrossRef]
55. Sharon, H. A detailed review on sole and hybrid solar chimney based sustainable ventilation, power generation, and potable water production systems. *Energy Nexus* **2023**, *10*, 100184. [CrossRef]
56. Liu, Y.; Ming, T.; Peng, C.; Wu, Y.; Li, W.; Richter, R.; Zhou, N. Mitigating air pollution strategies based on solar chimneys. *Sol. Energy* **2021**, *218*, 11–27. [CrossRef]
57. Mandal, D.K.; Goswami, P.; Pradhan, S.; Chakraborty, R.; Khan, N.A.; Bose, P. A numerical experimentation on fluid flow and heat transfer in a SCPP. *IOP Conf. Ser. Mater. Sci. Eng.* **2021**, *1080*, 012027. [CrossRef]
58. Mandal, D.K.; Pradhan, S.; Chakraborty, R.; Barman, A.; Biswas, N. Experimental investigation of a solar chimney power plant and its numerical verification of thermo-physical flow parameters for performance enhancement. *Sustain. Energy Technol. Assess.* **2022**, *50*, 101786.
59. Fluri, T.P. Turbine Layout for and Optimization of Solar Chimney Power Conversion Units. Ph.D. Thesis, University of Stellenbosch, Stellenbosch, South Africa, 2008.
60. Calder, R. *Leonardo and the Age of the Eye*; Heinemann: Singapore, 1970.
61. Pastohr, H. Thermodynamischmodellierung eines aufwindkraftwerkes (Thermodynamic Modeling of a Solar Chimney). Ph.D. Thesis, Civil Engineering, Bauhaus-Universität Weimar, Weimar, Germany, 2004.
62. Cabanyes, I. Las chimeneas solares (Solar chimneys). *La energía Eléctrica*. 1903.
63. Bernardes, M.A.S. Solar chimney power plants—Developments and advancements. In *Solar Energy*; Belmiloudi, A., Ed.; InTech: Rijeka, Croatia, 2011; pp. 171–186.

64. Günther, H. In *Hundert Jahren-Die Künftige Energieversorgung der Welt (In Hundred Years-Future Energy Supply of the World)*; Kosmos, Franckh'sche Verlagshandlung Stuttgart: Stuttgart, Germany, 1931.
65. Brenneis, R.J.; Johnson, E.P.; Shi, W.; Plata, D.L. Atmospheric- and Low-Level Methane Abatement via an Earth-Abundant Catalyst. *ACS Environ. Au.* **2022**, *2*, 223–231. [[CrossRef](#)]
66. Pasumarthi, N.; Sherif, S.A. Experimental and theoretical performance of a demonstration solar chimney model-Part II: Experimental and theoretical results and economic analysis. *Int. J. Energy Res.* **1998**, *22*, 443–461. [[CrossRef](#)]
67. Schlaich, J.; Bergemann, R.; Schiel, W.; Weinrebe, G. Sustainable electricity generation with solar updraft towers. *Struct. Eng. Int.* **2004**, *14*, 225–229. [[CrossRef](#)]
68. Schlaich, J.; Bergemann, R.; Schiel, W.; Weinrebe, G. Design of commercial solar updraft tower systems—Utilisation of solar induced convective flows for power generation. *J. Sol. Energy Eng. Trans. ASME* **2005**, *127*, 117–124. [[CrossRef](#)]
69. Haaf, W.; Friedrich, K.; Mayr, G.; Schlaich, J. Solar chimneys Part I, Principle and construction of the pilot plant in Manzanares. *Int. J. Sol. Energy* **1983**, *2*, 3–20. [[CrossRef](#)]
70. Castillo, M. A new solar chimney design to harness energy from the atmosphere. *Spirit. Enterp.* **1984**, *11*, 58–59.
71. Cao, Q.; Pui, D.Y.H.; Lipinski, W. A concept of a Novel Solar-Assisted Large-Scale Cleaning System (SALSCS) for Urban Air Remediation. *Aerosol Ad. Air Qual. Res.* **2015**, *15*, 1–10. [[CrossRef](#)]
72. Zhou, X.; Xu, Y.; Yuan, S.; Wu, C.; Zhang, H. Performance and potential of solar updraft tower used as an effective measure to alleviate Chinese urban haze problem. *Renew. Sustain. Energy Rev.* **2015**, *51*, 1499–1508. [[CrossRef](#)]
73. Ming, T.; Liu, W.; Caillol, S. Fighting global warming by climate engineering, is the Earth radiation management and the solar radiation management any option for fighting climate change? *Renew. Sustain. Energy Rev.* **2014**, *31*, 792–834. [[CrossRef](#)]
74. Jing, H.; Chen, Z.; Li, A. Experimental study of the prediction of the ventilation flow rate through solar chimney with large gap-to-height ratios. *Build. Environ.* **2015**, *89*, 150–159. [[CrossRef](#)]
75. Khanal, R.; Lei, C. Solar chimney—A passive strategy for natural ventilation. *Energy Build.* **2011**, *43*, 1811–1819. [[CrossRef](#)]
76. Das, P.; Chandramohan, V.P. CFD analysis on flow and performance parameters estimation of solar updraft tower (SUT) plant varying its geometrical configurations. *Energy Sources A* **2018**, *40*, 1532–1546. [[CrossRef](#)]
77. Shahi, D.V.V.; Gupta, A.; Nayak, V.S. CFD analysis of solar chimney wind power plant by Ansys Fluent. *Int. J. Technol. Res. Eng.* **2018**, *5*, 3746–3751.
78. Balijepalli, R.; Chandramohan, V.P.; Kirankumar, K. Development of a small-scale plant for a Solar chimney power plant (SCPP), a detailed fabrication procedure; experiments and performance parameters evaluation. *Renew. Energy* **2020**, *148*, 247–260. [[CrossRef](#)]
79. Nasraoui, H.; Driss, Z.; Ayadi, A.; Bouabidi, A.; Kchaou, H. Numerical and experimental study of the impact of conical chimney angle on the thermodynamic characteristics of a solar chimney power plant. *Proc. Inst. Mech. Eng. Part E* **2019**, *233*, 1185–1199. [[CrossRef](#)]
80. Yapici, E.Ö.; Ayli, E.; Nsaif, O. Numerical investigation on the performance of a small scale solar chimney power plant for different geometrical parameters. *J. Clean. Prod.* **2020**, *276*, 122908. [[CrossRef](#)]
81. Das, P.; Chandramohan, V.P. Performance characteristics of divergent chimney solar updraft tower plant. *Int. J. Energy Res.* **2020**, *45*, 1–16. [[CrossRef](#)]
82. Mandal, D.K.; Biswas, N.; Manna, N.K.; Benim, A.C. Impact of chimney divergence and sloped absorber on energy efficacy of a solar chimney power plant (SCPP). *Ain Shams Eng. J.* **2023**, *15*, 102390. [[CrossRef](#)]
83. Mandal, D.K.; Biswas, N.; Manna, N.K.; Gayen, D.; Benim, A.C. An application of Artificial Neural Network (ANN) for comparative performance assessment of solar chimney (SC) plant for green energy production. *Sci. Rep.* **2024**, *14*, 979. [[CrossRef](#)]
84. Cuce, P.M.; Cuce, E.; Sen, H. Improving electricity production in Solar chimney power plants with sloping ground design, an extensive CFD research. *J. Sol. Energy Res. Updates* **2020**, *7*, 122–131. [[CrossRef](#)]
85. Mandal, D.K.; Biswas, N.; Barman, A.; Chakraborty, R.; Manna, N.K. A novel design of absorber surface of solar chimney power plant (SCPP), Thermal assessment; exergy and regression analysis. *Sustain. Energy Technol. Assess.* **2023**, *56*, 103039. [[CrossRef](#)]
86. Biswas, N.; Mandal, D.K.; Manna, N.K.; Benim, A.C. Novel stair-shaped ground absorber for performance enhancement of solar chimney power plant. *Appl. Therm. Eng.* **2023**, *227*, 120466. [[CrossRef](#)]
87. Djimli, S.; Chaker, A.; Ajib, S.; Habka, M. Studying the possibility of a combined hybrid solar chimney power plant with a gas turbine. *Environ. Prog. Sustain. Energy* **2017**, *36*, 501–508. [[CrossRef](#)]
88. Fathi, N.; McDaniel, P.; Aleyasin, S.S.; Robinson, M.; Vorobieff, P.; Rodriguez, S.; Oliveira, C. Efficiency enhancement of solar chimney power plant by use of waste heat from nuclear power plant. *J. Clean. Prod.* **2018**, *180*, 407–416. [[CrossRef](#)]
89. Yazdi, M.H.; Solomin, E.; Fudholi, A.; Sopian, K.; Chong, P.L. Numerical analysis of the performance of a hybrid solar chimney system with an integrated external thermal source. *Therm. Sci. Eng. Prog.* **2021**, *26*, 101127. [[CrossRef](#)]
90. Liu, Q.; Cao, F.; Liu, Y.; Zhu, T.; Liu, D. Design and simulation of a solar chimney PV/T power plant in Northwest China. *Int. J. Photoenergy* **2018**, *2018*, 1478695. [[CrossRef](#)]
91. Habibollahzade, A. Employing photovoltaic/thermal panels as a solar chimney roof, 3E analyses and multi-objective optimization. *Energy* **2019**, *166*, 118–130. [[CrossRef](#)]
92. Ahmed, O.K.; Hussein, A.S.; Daoud, R.W.; Ali, Z.H. A new method to improve the performance of solar chimneys. *AIP Conf. Proc.* **2020**, *2213*, 020018.
93. Singh, A.P.; Kumar, A.; Akshayveer; Singh, O.P. Performance enhancement strategies of a hybrid solar chimney power plant integrated with photovoltaic panel. *Energy Conv. Manag.* **2020**, *218*, 113020. [[CrossRef](#)]

94. Hussam, W.K.; Salem, H.J.; Redha, A.M.; Khlefat, A.M.; Khatib, F.A. Experimental and numerical investigation on a hybrid solar chimney-photovoltaic system for power generation in Kuwait. *Energy Conv. Manag. X* **2022**, *15*, 100249. [[CrossRef](#)]
95. Li, H.; Yu, Y.; Niu, F.; Shafik, M.; Chen, B. Performance of a coupled cooling system with earth-to-air heat exchanger and solar chimney. *Renew. Energy* **2014**, *62*, 468–477. [[CrossRef](#)]
96. Mokrani, O.B.E.K.; Ouahrani, M.R.; Sellami, M.H.; Segni, L. Experimental investigations of hybrid, geothermal water/solar chimney power plant. *Energy Sources A* **2020**, 1–18. [[CrossRef](#)]
97. Habibollahzade, A.; Houshfar, E.; Ashjaee, M.; Ekradi, K. Continuous power generation through a novel solar/geothermal chimney system, technical/cost analyses and multi-objective particle swarm optimization. *J. Clean. Prod.* **2021**, *283*, 124666. [[CrossRef](#)]
98. Akbarzadeh, A.; Johnson, P.; Singh, R. Examining potential benefits of combining a chimney with a salinity gradient solar pond for production of power in salt affected areas. *Sol. Energy* **2009**, *83*, 1345–1359. [[CrossRef](#)]
99. Assem, A. Hydro and solar-pond-chimney power scheme for Qattara Depression. *Egypt. Int. J. Water Resour. Environ. Eng.* **2014**, *6*, 12–18. [[CrossRef](#)]
100. Kiwan, S.; Al-Nimr, M.; Salim, I. A hybrid solar chimney/photovoltaic thermal system for direct electric power production and water distillation. *Sustain. Energy Technol. Assess.* **2020**, *38*, 100680. [[CrossRef](#)]
101. Rahdan, P.; Kasaeian, A.; Yan, W.M. Simulation and geometric optimization of a hybrid system of solar chimney and water desalination. *Energy Conv. Manag.* **2021**, *243*, 114291. [[CrossRef](#)]
102. Tawalbeh, M.; Mohammed, S.; Alnaqbi, A.; Alshehhi, S.; Al-Othman, A. Analysis for hybrid photovoltaic/solar chimney seawater desalination plant, A CFD simulation in Sharjah; United Arab Emirates. *Renew. Energy* **2023**, *202*, 667–685. [[CrossRef](#)]
103. Zandian, A.; Ashjaee, M. The thermal efficiency improvement of a steam Rankine cycle by innovative design of a hybrid cooling tower and a solar chimney concept. *Renew. Energy* **2013**, *51*, 465–473. [[CrossRef](#)]
104. Zou, Z.; He, S. Modeling and characteristics analysis of hybrid cooling-tower solar-chimney system. *Energy Conv. Manag.* **2015**, *95*, 59–68. [[CrossRef](#)]
105. Khanal, R.; Lei, C. A numerical investigation of buoyancy induced turbulent air flow in an inclined passive wall solar chimney for natural ventilation. *Energy Build.* **2015**, *93*, 217–226. [[CrossRef](#)]
106. Nasri, F.; Alqurashi, F.; Nciri, R.; Ali, C. Design and simulation of a novel solar air-conditioning system coupled with solar chimney. *Sustain. Cities Soc.* **2018**, *40*, 667–676. [[CrossRef](#)]
107. Vargas-López, R.; Xamán, J.; Hernández-Pérez, I.; Arce, J.; Zavala-Guillén, I.; Jiménez, M.J.; Heras, M.R. Mathematical models of solar chimneys with a phase change material for ventilation of buildings, A review using global energy balance. *Energy* **2019**, *170V*, 683–708. [[CrossRef](#)]
108. Maghrabie, M.H.; Abdelkareem, M.A.; Elsaid, K.; Sayed, E.T.; Radwan, A.; Rezk, H.; Wiberfore, T.; Abo-Khali, A.G.; Olab, A.G. A review of solar chimney for natural ventilation of residential and non-residential buildings. *Sustain. Energy Technol. Assess.* **2022**, *52*, 102082. [[CrossRef](#)]
109. Alyea, F.; Cunnold, D.; Prinn, R. Meteorological constraints on tropospheric halocarbon and nitrous oxide destructions by siliceous land surfaces. *Atmos. Environ.* **1978**, *12*, 1009–1011. [[CrossRef](#)]
110. Pierotti, D.; Rasmussen, L.; Rasmussen, R. The Sahara as a possible sink for trace gases. *Geophys. Res. Lett.* **1978**, *5*, 1001–1004. [[CrossRef](#)]
111. George, C.; Ammann, M.; D’Anna, B.; Donaldson, D.J.; Nizkorodov, S.A. Heterogeneous photochemistry in the atmosphere. *Chem. Rev.* **2015**, *115*, 4218–4258. [[CrossRef](#)] [[PubMed](#)]
112. de Richter, R.; Caillol, S. Fighting global warming: The potential of photocatalysis against CO₂, CH₄, N₂O, CFC, tropospheric O₃, BC and other major contributors to climate change. *J. Photochem. Photobiol. C Photochem. Rev.* **2011**, *12*, 1–19. [[CrossRef](#)]
113. de Richter, R.K.; Ming, T.; Caillol, S. Fighting global warming by photocatalytic reduction of CO₂ using giant photocatalytic reactors. *Renew. Sustain. Energy Rev.* **2013**, *19*, 82–100. [[CrossRef](#)]
114. de Richter, R.; Ming, T.; Davies, P.; Liu, W.; Caillol, S. Removal of non-CO₂ greenhouse gases by Large-scale atmospheric solar photocatalysis. *Prog. Energy Comb. Sci.* **2017**, *60*, 68–96. [[CrossRef](#)]
115. Zhao, G.Q.; Hu, J.; Long, X.; Zou, J.; Yu, J.G.; Jiao, F.P. A Critical Review on Black Phosphorus-Based Photocatalytic CO₂ Reduction Application. *Small* **2021**, *17*, 2102155. [[CrossRef](#)]
116. Thampi, K.R.; Kiwi, J.; Graetzel, M. Methanation and photo-methanation of carbon dioxide at room temperature and atmospheric pressure. *Nature* **1987**, *327*, 506. [[CrossRef](#)]
117. Anpo, M.; Chiba, K. Photocatalytic reduction of CO₂ on anchored titanium oxide catalysts. *J. Mol. Catal.* **1992**, *74*, 207–212. [[CrossRef](#)]
118. Anpo, M.; Yamashita, H.; Ichihashi, Y.; Ehara, S. Photocatalytic reduction of CO₂ with H₂O on various titanium oxide catalysts. *J. Electroanal. Chem.* **1995**, *396*, 21. [[CrossRef](#)]
119. Koci, K.; Obalova, L.; Lacny, Z. Photocatalytic reduction of CO₂ over TiO₂ based catalysts. *Chem. Pap.* **2008**, *62*, 1–9. [[CrossRef](#)]
120. Wang, B.; Chen, W.; Song, Y.; Li, G.; Wei, W.; Fang, J.; Sun, Y. Recent progress in the photocatalytic reduction of aqueous carbon dioxide. *Catal. Today* **2018**, *311*, 23–39. [[CrossRef](#)]
121. Khalil, M.; Gunlazuardi, J.; Ivandini, T.A.; Umar, A. Photocatalytic conversion of CO₂ using earth-abundant catalysts: A review on mechanism and catalytic performance. *Renew. Sustain. Energy Rev.* **2019**, *113*, 109246. [[CrossRef](#)]

122. Alkhatib, I.I.; Garlisi, C.; Pagliaro, M.; Al-Ali, K.; Palmisano, G. Metal-organic frameworks for photocatalytic CO₂ reduction under visible radiation: A review of strategies and applications. *Catal. Today* **2020**, *340*, 209–224. [[CrossRef](#)]
123. Trickett, C.A.; Helal, A.; Al-Maythaly, B.A.; Yamani, Z.H.; Cordova, K.E.; Yaghi, O.M. The chemistry of metal-organic frameworks for CO₂ capture, regeneration and conversion. *Nat. Rev. Mater.* **2017**, *2*, 17045. [[CrossRef](#)]
124. Xiao, J.-D.; Jiang, H.-L. Metal-organic frameworks for photocatalysis and photothermal catalysis. *Acc. Chem. Res.* **2019**, *52*, 356–366. [[CrossRef](#)]
125. Yang, Q.; Luo, M.; Liu, K.; Cao, H.; Yan, H. Covalent organic frameworks for photocatalytic applications. *Appl. Catal.* **2020**, *276*, 119174. [[CrossRef](#)]
126. Zhi, Y.; Wang, Z.; Zhang, H.-L.; Zhang, Q. Recent progress in metal-free covalent organic frameworks as heterogeneous catalysts. *Small* **2020**, *16*, 2001070. [[CrossRef](#)] [[PubMed](#)]
127. Ye, L.; Deng, Y.; Wang, L.; Xie, H.; Su, F. Bismuth-based photocatalysts for solar photocatalytic carbon dioxide conversion. *ChemSusChem* **2019**, *12*, 3671–3701. [[CrossRef](#)]
128. Zhang, X.; Yuan, X.; Jiang, L.; Zhang, J.; Yu, H.; Wang, H.; Zeng, G. Powerful combination of 2D g-C₃N₄ and 2D nanomaterials for photocatalysis: Recent advances. *Chem. Eng. J.* **2020**, *390*, 124475. [[CrossRef](#)]
129. Lee, Y.; Kim, S.; Kang, J.; Cohen, S. Photocatalytic CO₂ reduction by a mixed metal (Zr/Ti), mixed ligand metal-organic framework under visible light irradiation. *Chem. Commun.* **2015**, *51*, 5735–5738. [[CrossRef](#)] [[PubMed](#)]
130. Huabin, Z.; Wei, J.; Dong, J.; Liu, G.; Shi, L.; An, P. Efficient visible-light-driven carbon dioxide reduction by a single-atom implanted metal-organic framework. *Angew. Chem.* **2016**, *128*, 14522–14526.
131. Fu, Y.; Zhu, X.; Huang, L.; Zhang, X.; Zhang, F.; Zhu, W. Azine-based covalent organic frameworks as metal-free visible light photocatalysts for CO₂ reduction with H₂O. *Appl. Catal. B* **2018**, *239*, 46–51. [[CrossRef](#)]
132. Lu, M.; Li, Q.; Liu, J.; Zhang, F.-M.; Zhang, L.; Wang, J.-L. Installing earth-abundant metal active centers to covalent organic frameworks for efficient heterogeneous photocatalytic CO₂ reduction. *Appl. Catal. B* **2019**, *254*, 624–633. [[CrossRef](#)]
133. Wang, J.C.; Yao, H.C.; Fan, Z.Y.; Zhang, L.; Wang, J.S.; Zang, S.Q.; Li, Z.J. Indirect Z-scheme BiOI/g-C₃N₄ photocatalysts with enhanced photoreduction CO₂ activity under visible light irradiation. *ACS Appl. Mater. Interfaces* **2016**, *8*, 3765–3775. [[CrossRef](#)]
134. Xia, P.; Zhu, B.; Yu, J.; Cao, S.; Jaroniec, M. Ultra-thin nanosheet assemblies of graphitic carbon nitride for enhanced photocatalytic CO₂ reduction. *J. Mater. Chem.* **2017**, *5*, 3230–3238. [[CrossRef](#)]
135. Kumar, A.; Kumar, P.; Borkar, R.; Bansiwala, A.; Labhsetwar, N.; Jain, S.L. Metal-organic hybrid: Photoreduction of CO₂ using graphitic carbon nitride supported heteroleptic iridium complex under visible light irradiation. *Carbon* **2017**, *123*, 371–379. [[CrossRef](#)]
136. Formenti, M.; Juillet, F.; Meriaudeau, P.; Teichner, S.J.; Vergnon, P.J. Preparation in a hydrogen-oxygen flame of ultrafine metal oxide particles. Oxidative properties toward hydrocarbons in the presence of ultraviolet radiation. *Colloid. Interface Sci.* **1972**, *39*, 79. [[CrossRef](#)]
137. Djeghri, N.; Formenti, M.; Juillet, F.; Teichner, S.J. Photointeraction on the surface of titanium dioxide between oxygen and alkanes. *Faraday Discuss. Chem. Soc.* **1974**, *58*, 185.
138. Kaliaguine, S.L.; Shelimov, B.N.; Kazansky, V.B. Reactions of methane and ethane with hole centers. *J. Catal.* **1978**, *55*, 384. [[CrossRef](#)]
139. Krishna, V.; Kamble, V.S.; Selvam, P.; Gupta, N.M. Sunlight-assisted photocatalytic oxidation of methane over uranyl-anchored MCM-41. *Catal. Lett.* **2004**, *98*, 113. [[CrossRef](#)]
140. In, S.I.; Nielsen, M.G.; Vesborg, P.C.K.; Hou, Y.; Abrams, B.L.; Henriksen, T.R.; Hansen, O.; Chorkendorff, I.B. Photocatalytic methane decomposition over vertically aligned transparent TiO₂ nanotube arrays. *Chem. Commun.* **2011**, *47*, 2613. [[CrossRef](#)]
141. Pan, X.; Chen, X.; Yi, Z. Photocatalytic oxidation of methane over SrCO₃ decorated SrTiO₃ nanocatalysts via a synergistic effect. *Phys. Chem. Chem. Phys.* **2016**, *18*, 31400–31409. [[CrossRef](#)]
142. Chen, X.; Li, Y.; Pan, X.; Cortie, D.; Huang, X.; Yi, Z. Photocatalytic oxidation of methane over silver decorated zinc oxide nanocatalysts. *Nat. Commun.* **2016**, *7*, 1–8. [[CrossRef](#)]
143. Wei, J.; Yang, J.; Wen, Z.; Dai, J.; Li, Y.; Yao, B. Efficient photocatalytic oxidation of methane over β-Ga₂O₃/activated carbon composites. *RSC Adv.* **2017**, *7*, 37508–37521. [[CrossRef](#)]
144. Li, Z.H.; Boda, M.A.; Pan, X.Y.; Yi, Z.G. Photocatalytic oxidation of small molecular hydrocarbons over ZnO nanostructures, the difference between methane and ethylene and the impact of polar and nonpolar facets. *ACS Sustain. Chem. Eng.* **2019**, *7*, 19042–19049. [[CrossRef](#)]
145. Li, Z.; Pan, X.; Yi, Z. Photocatalytic oxidation of methane over CuO-decorated ZnO nanocatalysts. *J. Mater. Chem.* **2019**, *7*, 469–475. [[CrossRef](#)]
146. Ebitani, K.; Morokuma, M.; Kim, J.H.; Morikawa, A. Photocatalytic decomposition of nitrous oxide on Cu-ion-containing ZSM-5 catalyst. *J. Catal.* **1993**, *141*, 725–728. [[CrossRef](#)]
147. Ebitani, K.; Morokuma, M.; Kim, J.H.; Morikawa, A. Photocatalytic decomposition of dinitrogen oxide on Cu-containing ZSM-5 catalyst. *J. Chem. Soc. Faraday Trans.* **1994**, *90*, 377–381. [[CrossRef](#)]
148. Ebitani, K.; Hirano, Y.; Morikawa, A. Rare earth ions as heterogeneous photocatalysts for the decomposition of dinitrogen monoxide (N₂O). *J. Catal.* **1995**, *157*, 262–265. [[CrossRef](#)]
149. Kudo, A.H.; Nagayoshi, H. Photocatalytic reduction of N₂O on metal-supported TiO₂ powder at room temperature in the presence of H₂O and CH₃OH vapor. *Catal. Lett.* **1998**, *52*, 109. [[CrossRef](#)]

150. Matsuoka, M.; Anpo, M. Local structures, excited states, and photocatalytic reactivities of highly dispersed catalysts constructed within zeolites. *J. Photochem. Photobiol. C* **2003**, *3*, 225–252. [CrossRef]
151. Guarino, M.; Annamaria, C.; Marco, P. Photocatalytic TiO₂ coating—To reduce ammonia and greenhouse gases concentration and emission from animal husbandries. *Bioresour. Technol.* **2008**, *99*, 2650. [CrossRef]
152. Matsuoka, M.; Ju, W.-S.; Yamashita, H.; Anpo, M. Investigations on the local structure of Ag⁺/ZSM-5 catalysts and their photocatalytic reactivities for the decomposition of N₂O at 298 K. *J. Synchrotron Radiat.* **2001**, *8*, 613–615. [CrossRef] [PubMed]
153. Ju, W.-S.; Matsuoka, M.; Anpo, M. Incorporation of silver (I) ions within zeolite cavities and their photocatalytic reactivity for the decomposition of N₂O into N₂ and O₂. *Int. J. Photoenergy* **2003**, *5*, 17–19. [CrossRef]
154. Rakhmawaty, D.; Matsuoka, M.; Anpo, M. Photocatalytic decomposition of N₂O in the presence of CO on Ti/USY photocatalysts. In Proceedings of the International Seminar on Chemistry, Jatinangor, Indonesia, 30–31 October 2008; ISBN 978-979-18962-0-7. pp. 342–345.
155. Kočí, K.; Krejčíková, S.; Šolcová, O.; Obalová, L. Photocatalytic decomposition of N₂O on Ag-TiO₂. *Catal. Today* **2012**, *191*, 134–137. [CrossRef]
156. Kočí, K.; Matějová, L.; Obalová, L.; Čapek, L.; Wu, J.C. Preparation, characterization and photocatalytic performance of TiO₂ prepared by using pressurized fluids in CO₂ reduction and N₂O decomposition. *J. Sol.-Gel. Sci. Technol.* **2015**, *76*, 621–629. [CrossRef]
157. Matějov, L.; Šihor, M.; Brunátová, T.; Ambrožová, N.; Reli, M.; Čapek, L.; Obalová, L.; Kočí, K. Microstructure-performance study of cerium-doped TiO₂ prepared by using pressurized fluids in photocatalytic mitigation of N₂O. *Res. Chem. Int.* **2015**, *41*, 9217–9231. [CrossRef]
158. Tanaka, K.; Hisanaga, T. Photodegradation of chlorofluorocarbon alternatives on metal oxide. *Sol. Energy* **1994**, *52*, 447–450. [CrossRef]
159. Tennakone, K.; Wijayantha, K.G.U. Photocatalysis of CFC degradation by titanium dioxide. *Appl. Catal. B Environ.* **2005**, *57*, 9–12. [CrossRef]
160. Minami, W.; Hee-Joon, K. Decomposition of halocarbons using TiO₂ photocatalyst. *Kagaku Kogaku Ronbunshu* **2006**, *32*, 310–313. [CrossRef]
161. Tan, D.; Zhou, X.; Xu, Y.; Wu, C.; Li, Y. Environmental; health and economic benefits of using urban updraft tower to govern urban air pollution. *Renew. Sustain. Energy Rev.* **2017**, *77*, 1300–1308. [CrossRef]
162. Cao, Q.; Thomas, H.; Kuehn, T.H.; Shen, L.; Chen, S.C.; Zhang, N.; Huang, Y.; Cao, J.; Pui, D.Y.H. Urban-scale SALSCS: Part I: Experimental evaluation and numerical modeling of a demonstration unit. *Aerosol Air Qual. Res.* **2018**, *18*, 2865–2878. [CrossRef]
163. Ghanbari, M.; Rezazadeh, G. Giant chimney for air ventilation of metropolises. *Atmos. Pollut. Res.* **2019**, *10*, 462–473. [CrossRef]
164. Daghistani, F.F. Solar chimney street-lighting pole for ventilating polluted urban areas. *Sustain. Cities Soc.* **2021**, *72*, 103057. [CrossRef]
165. Hachicha, A.A.; Abo-Zahhad, E.M.; Oh, S.; Rahman, S.M.A. Numerical investigation and optimization of a novel hybrid solar chimney for air pollution mitigation and clean electricity generation. *Appl. Therm. Eng.* **2023**, *226*, 120271. [CrossRef]
166. Yoo, S.; Oh, S.; Hachicha, A.A. Numerical simulation and performance evaluation of filter-equipped solar chimney power plants. *Appl. Therm. Eng.* **2023**, *218*, 119284. [CrossRef]
167. Gong, T.; Ming, T.; Huang, X.; de Richter, R. Numerical analysis on a solar chimney with an inverted U-type cooling tower to mitigate urban air pollution. *Sol. Energy* **2017**, *147*, 68–82. [CrossRef]
168. National Oceanic and Atmospheric Administration (NOAA). 2010. Available online: <http://www.esrl.noaa.gov/gmd/ccgg/trends/global.html> (accessed on 7 September 2023).
169. Wu, J.C.S. Renewable energy from the photocatalytic reduction of CO₂ with H₂O. In *Environmentally Benign Photocatalysts, Applications of Titanium Oxide-Based Materials (Nanostructurescience & Technology)*; Anpo, M., Kamat, P., Eds.; Springer: Berlin/Heidelberg, Germany, 2010; Chapter 28.
170. Roy, S.C.; Varghese, O.K.; Paulose, M.; Grimes, C.A. Toward solar fuels, photocatalytic conversion of carbon dioxide to hydrocarbons. *ACS Nano* **2010**, *4*, 1259–1278. [CrossRef]
171. Usubharatana, P.; McMartin, D.; Veawab, A.; Tontiwachwuthikul, P. Photocatalytic process for CO₂ emission reduction from industrial flue gas streams. *Indust. Eng. Chem. Res.* **2006**, *45*, 2558–2568. [CrossRef]
172. Magesh, G.; Viswanathan, B.; Viswanath, R.P.; Varadarajan, T.K. Photocatalytic routes for chemicals. In *Photo/Electrochemistry & Photobiology in the Environment*; Kaneco, S., Viswanathan, B., Katsumata, H., Eds.; Energy Fuel: Kerala, India; Research Signpost: Thiruvananthapuram, India, 2007; Chapter 11; 37p.
173. Indrakanti, V.P.; Kubicki, J.D.; Schobert, H.H. Photoinduced activation of CO₂ on Ti-based heterogeneous catalysts, current state; chemical physics-based insights and outlook. *Energy Environ. Sci.* **2009**, *2*, 745–758. [CrossRef]
174. Zhang, Y.; Yang, R.; Zhao, R. A model for analyzing the performance of photocatalytic air cleaner in removing volatile organic compounds. *Atmosph. Environ.* **2003**, *37*, 3395–3399. [CrossRef]
175. Ming, T.; de Richter, R.; Sheng, S.; Caillol, S. Fighting global warming by greenhouse gas removal, destroying atmospheric nitrous oxide thanks to synergies between two breakthrough technologies. *Environ. Sci. Pollut. Res.* **2016**, *23*, 6119–6138. [CrossRef]
176. Ming, T.; Gui, H.; Shi, T.; Xiong, H.; Wu, Y.; Shao, Y.; Li, W.; Lu, X.; de Richter, R. Solar chimney power plant integrated with a photocatalytic reactor to remove atmospheric methane: A numerical analysis. *Sol. Energy* **2021**, *226*, 101–111. [CrossRef]

177. Xiong, H.; Ming, T.; Wu, Y.; Wang, C.; Chen, Q.; Li, W.; Mu, L.; de Richter, R.; Yaun, Y. Numerical analysis of solar chimney power plant integrated with CH₄. *Energy* **2022**, *201*, 678–690.
178. United Nations Environment Programme. Environmental effects of ozone depletion and its interactions with climate change: Progress report, 2015. *Photochem. Photobiol. Sci.* **2016**, *15*, 141–174. [[CrossRef](#)]

Disclaimer/Publisher's Note: The statements, opinions and data contained in all publications are solely those of the individual author(s) and contributor(s) and not of MDPI and/or the editor(s). MDPI and/or the editor(s) disclaim responsibility for any injury to people or property resulting from any ideas, methods, instructions or products referred to in the content.